COLLOIDAL STABILIZATION OF LTA TYPE ZEOLITES IN ETHANOL-WATER MIXTURES

A THESIS SUBMITTED TO
THE GRADUATE SCHOOL OF NATURAL AND APPLIED SCIENCES
OF
MIDDLE EAST TECHNICAL UNIVERSITY

BY

OĞUZ GÖZCÜ

IN PARTIAL FULFILLMENT OF THE REQUIREMENTS
FOR
THE DEGREE OF MASTER OF SCIENCE
IN
METALLURGICAL AND MATERIALS ENGINEERING

JANUARY 2020

Approval of the thesis:

COLLOIDAL STABILIZATION OF LTA TYPE ZEOLITES IN ETHANOL-WATER MIXTURES

submitted by **OĞUZ GÖZCÜ** in partial fulfillment of the requirements for the degree of **Master of Science in Metallurgical and Materials Engineering Department, Middle East Technical University** by,

Prof. Dr. Halil Kalıpçılar
Dean, Graduate School of **Natural and Applied Sciences** _____

Prof. Dr. Cemil Hakan Gür
Head of Department, **Met. and Mat. Eng.** _____

Assist. Prof. Dr. Simge Çınar
Supervisor, **Met. and Mat. Eng., METU** _____

Examining Committee Members:

Prof. Dr. Caner Durucan
Met. and Mat. Eng., METU _____

Assist. Prof. Dr. Simge Çınar
Met. and Mat. Eng., METU _____

Assist. Prof. Dr. Emre Büküşoğlu
Chemical Engineering, METU _____

Prof. Dr. Bora Maviş
Mechanical Engineering, Hacettepe University _____

Prof. Dr. H. Emrah Ünalan
Met. and Mat. Eng., METU _____

Date: 15.01.2020

I hereby declare that all information in this document has been obtained and presented in accordance with academic rules and ethical conduct. I also declare that, as required by these rules and conduct, I have fully cited and referenced all material and results that are not original to this work.

Name, Surname: Oğuz Gözcü

Signature:

ABSTRACT

COLLOIDAL STABILIZATION OF LTA TYPE ZEOLITES IN ETHANOL-WATER MIXTURES

Gözcü, Oğuz
Master of Science, Metallurgical and Materials Engineering
Supervisor: Assist. Prof. Dr. Simge Çınar

January 2020, 70 pages

Zeolites are promising materials for various applications because of their uniform pores at the nano- and micron- scales as well as their chemical and surface properties. In recent years, fabrication of the complex shape zeolites and nano-sized zeolites has been attracting attention to increase the efficiency in zeolite applications. Since conventional zeolite production techniques are not suitable for the fabrication of such zeolites, the use of techniques such as electrospinning, electrophoretic deposition, and robocasting has been suggested. Those techniques generally require storage, transportation, or dispersion of the zeolite powders in a pure or mixed liquid media often with a carrier polymer, so the dispersion characteristics of zeolites in liquid media are critical for such processes. However, there are only a few studies in literature discussing the stabilization of zeolite powders. Besides, the stabilization of zeolites in mixed solvents and the presence of polymers is not a trivial task. The aim of this study is, therefore, to investigate the dispersion characteristic of zeolites in mixed solvents and discuss the applicability of the available stabilization techniques for zeolite powders in mixed solvents with various concentrations, and in the presence of polymeric carriers. To this end, common LTA zeolites were used, and its dispersion behavior was investigated in ethanol-water mixtures with various concentrations (30:70, 40:60, and 50:50 wt%). Even though zeolite powders were stable in water-rich

solutions, increasing ethanol concentrations required the use of additives for dispersion of zeolite powders. Applicability of electrostatic and steric/electrosteric stabilization mechanisms was discussed, and the use of steric/electrosteric stabilization with non-ionic additives was preferred in order to prevent the changes in the chemical structure of zeolites in ionic solutions. The effects of various additives were investigated using a sedimentation test, zeta potential measurements, and ATR-FTIR analysis. High molecular weight PVP was used as a carrier polymer, which worsened the stability of zeolite powders. The rate of LTA zeolite sedimentation in the presence of carrier polymer was slowed down using dispersants. The effect of such an improvement was also demonstrated with the change in dispersion quality of zeolite films produced by spin coating of PVP containing mixed solvent zeolite suspensions.

Keywords: Colloidal stabilization, LTA Zeolite, ethanol-water mixture, dispersion of zeolites, spin coating of LTA zeolites

ÖZ

LTA ZEOLİTLERİNİN ETANOL-SU KARIŞIMI İÇERİSİNDEKİ KOLLOİDAL STABİLİZASYONU

Gözcü, Oğuz
Yüksek Lisans, Metalurji ve Malzeme Mühendisliği
Tez Danışmanı: Dr. Öğr. Üyesi Simge Çınar

Ocak 2020, 70 sayfa

Zeolitler, nano ve mikron ölçeğindeki homojen gözeneklerinin yanı sıra, kimyasal ve yüzey özellikleri nedeniyle çeşitli uygulamalar için umut vaat eden malzemelerdir. Son zamanlarda, zeolit uygulamalarının verimliliğini arttırmak için kompleks şekilde ve nano boyutta zeolit üretimi önem kazanmıştır. Geleneksel zeolit üretim metotları yukarıda bahsedilen zeolit şekilleri ve boyutlat için uygun olmadığından, elektro eğirme, elektrikle devinimli bırakıntı, robo-döküm ve benzeri yöntemler bu tarz zeolit yapıların üretimi için önerilmektedir. Bu teknikler genellikle zeolit tozlarının taşıyıcı polimer içeren sıvı bir ortamda depolanmasını, taşınmasını ve dağıtılmasını gerektirir. stabil ettiği gözlenmiştir. Bu çalışmanın amacı, karışık çözücülerdeki zeolitlerin dispersiyon karakteristiğini araştırmak ve çeşitli konsantrasyonlardaki karışık çözücülerde zeolit tozlarına stabilizasyon mekanizmalarının uygulanabilirliğini taşıyıcı polimerler içinde tartışmaktır. Bu amaçla, bu tezde yaygın olarak kullanılan LTA zeolit tozları seçildi ve bu tozların çeşitli etanol-su konsantrasyonlarındaki çözeltilerdeki (ağırlıkça %30:70, 40:60 ve 50:50) dispersiyon davranışı araştırıldı. Zeolit tozları, su açısından zengin çözeltilerde stabil olmasına rağmen artan etanol konsantrasyonlarıyla beraber zeolit tozlarının dağıtılması için katkı maddelerinin kullanılması gerekmiştir. Elektrostatik ve sterik / elektrosterik stabilizasyon mekanizmalarının zeolit süspansiyonlarına uygulanabilirliği tartışıldı ve iyonik

çözeltilerdeki zeolitlerin kimyasal yapısındaki değişiklikleri önlemek için iyonik olmayan katkı maddeleri ile sterik / elektrosterik stabilizasyonun kullanılması tercih edildi. Çeşitli katkı maddelerinin etkilerini görmek için sedimantasyon testi, zeta potansiyel ölçümleri ve ATR-FTIR analizleri yapıldı. Yüksek moleküler ağırlıklı PVP taşıyıcı polimer olarak kullanıldı. PVP polimerinin zeolit tozlarının stabilitesini kötüleştirdiği gözlemlendi ve PVP polimeri varlığındaki LTA zeolit tozlarının sedimantasyon hızı, dağıtıcılar kullanılarak yavaşlatıldı. Bu kimyasalların karışık çözücülerdeki PVP içeren zeolit süspansiyonları üzerindeki etkisi spin kaplama tekniği ile üretilen zeolit filmlerle gösterilmiştir.

Anahtar Kelimeler: Kolloidal stabilizasyon, LTA zeolit, etanol-su karışımı, zeolitlerin dağılması, LTA zeolitlerin spin kaplanması

To my beloved family

ACKNOWLEDGEMENTS

First and foremost, I would like to thank my supervisor, Simge ÇINAR, for her guidance and great support through the study with all the ups and downs. I considered myself very lucky to have a supervisor who responded to my questions and extended my knowledge.

I am particularly thankful to Bayram Yıldız, Utkucan Kayacı their help and assistance in many fields of study. I am surely grateful to Bersu Baştuğ Azer for helping me FTIR analysis in this study and her support.

I am particularly thanks to Prof. Dr. Andreas Kaiser and Assoc. Prof. Dr. Angela Zhang for all priceless advice and teaching me many detailed scientific aspects during my stay at Denmark Technical University, and I am also thanking them for providing zeolite powders.

I would like to thankful to Prof. Dr. Macit Özenbaş, Prof. Dr. Caner Durucan, and Prof. Dr. Bora Maviş for opening the use of lab apparatus.

My thanks are extended to my close friends: Tolga Han Ulucan, Gökberk Demirok, Hüseyin Can Çamiçi, Münevver Güllü, Ender Eryılmaz, Umutcan Önel, Hakan Yeter, and Ezgi Şahin.

Finally, I must express my very profound gratitude to my parents and brother for providing me with unfailing support and continuous encouragement throughout my years of study and through the process of researching and writing this thesis. This accomplishment would not have been possible without them.

TABLE OF CONTENTS

LIST OF TABLES

TABLES

LIST OF FIGURES

FIGURES

LIST OF ABBREVIATIONS

ABBREVIATIONS

PVP: Poly(vinylpyrrolidone)

PAA: Poly (acrylic acid)

CTAB: Hexadecyltrimethylammonium bromide

SLS: Sodium lauryl sulfate

PEG: Poly (ethylene glycol)

MW: Molecular Weight

CHAPTER 1

INTRODUCTION

Zeolites, three-dimensional ordered porous aluminosilicate minerals are used in a variety of commercial applications such as membranes, catalysts, and structural applications because of their unique properties: highly ordered nano- and micro-porous structure and versatile range of oxide networks, determining the chemical and surface properties of the structure [1]. The ordered porous structure and surface properties of zeolites provide higher flux and selectivity; thus, zeolites are commonly used as membranes in gas sensing [2], biogas separation [3], and water softening [4].

LTA type zeolite is one of the oldest synthetic zeolites, which is commercialized, and its properties are well studied applications as adsorbent and catalyst, particularly for adsorption of gases [5,6]. LTA type zeolite was selected as a model zeolite in this study because of its extensive use.

By technological developments and an increase in demands, the need for highly efficient zeolite products became urgent. However, the efficiency of currently available zeolites is limited due to their shapes, accessibility of the reaction sites, and reliability [7,8]. The efficiency of zeolites can be increased with the use of nano-sized powders and complex shape structures such as nano-fibers, nano-composites, monoliths or multichannel tubes, etc. [9]. Fabrication of such structures can also extend the application areas of zeolites. However, it is not straightforward to produce complex shaped zeolite structures via the conventional production methods, namely direct synthesis, seeding of zeolite crystals or coating, etc. [10,11]. Therefore, more complex production methods such as electrospinning, electrophoretic deposition (EPD), or robocasting are required [12–14]. The production of the nano-sized and complex shape zeolite structures such as monoliths, fibers, or monolith fibers has been popular in order to boost the efficiency of the zeolite shape. The monolith structures

have recently been produced via freeze casting, robocasting, and slip casting techniques [15–17]. The production techniques generally require zeolite suspensions powders in liquid media and viscous polymer carriers such as PVP or PVA [18–20]. These production methods also commonly require the use of dispersant or stabilizer.

The shaping of zeolites via colloidal processing has provided advantages of easy preparation, high quality, and scalability. Furthermore, mixed solvent media are started to be commonly used for various shaping methods since it enables the adjustments of viscosity, and many other process parameters [21–23]. Despite the importance of colloidal processing, the dispersion behavior of zeolite powders in suspensions is commonly overlooked. The stability of the particles could be vital because the agglomeration of powders in liquid media causes the heterogeneity in end product properties. Therefore, the homogeneous dispersion of the zeolite powders in liquid media plays a crucial role in obtaining homogeneous and defect-free zeolite products.

For this reason, the aim of this thesis is to investigate the dispersion behavior of zeolite powders in various environments and to systematically evaluate the available stabilization mechanisms for conditions where zeolite powders are agglomerated. In this study, the dispersion behavior of the LTA zeolite powders in the ethanol:water mixtures in the absence/presence of the high molecular weight PVP were studied. LTA was selected due to its wide use. Ethanol-water was selected as mixed media since water is one of the most abundant, cheap, and environmentally friendly solvent. Ethanol was used since its polarity, volatility in the suspension [24,25]. If the suspensions are not stable, then there is needed to apply colloidal stabilization mechanisms to zeolite suspensions. Three main stabilization mechanisms as electrostatic, steric, and electrosteric were studied in this study and all mechanisms were evaluated for dispersion of LTA zeolites in ethanol-water mixtures [26]. The effect of dispersants on stabilization of LTA zeolites was investigated using sedimentation tests, zeta potential measurements, and ATR-FTIR analysis.

This thesis mainly consisted of four chapters. In Chapter 2, introductory information and recent literature on LTA zeolites and fabrication of the zeolite structures using colloidal processing were scrutinized. The experimental details on the suspension preparation and characterization of the powders and suspensions used were present in Chapter 3. In Chapter 4, as-received zeolite powders characteristics were investigated and the procedures to prepare powders for dispersion studies were present. Then, the dispersion quality of the treated zeolite powders in the ethanol:water mixtures was investigated. For the unstable suspensions, electrostatic, and steric/electrosteric stabilization mechanisms were applied to prevent the agglomeration of particles in the medium. For this reason, the effect of suspension pH, the use of anionic, cationic, zwitterionic, and non-ionic dispersants were investigated. Then, the effect of the high molecular weight PVP polymer on the dispersion behavior of the suspensions was studied. The similar stabilization route mentioned above was followed for PVP containing suspensions. Finally, spin-coating was selected as a case study to demonstrate how stabilization methods affect the quality of fabricated zeolite films.

CHAPTER 2

LITERATURE REVIEW

2.1. Colloidal Stability

A solid particle with size ranging between 1 nm to few μm in fluids is considered as a colloidal particle. At about this size range, the particles can suspend in a liquid media because thermal motion (kT), i.e. counteracting diffusion behavior, can balance the gravitational force [27]. The gravitational force proportionally increases with increasing particle size, while thermal motion remains almost constant. Therefore, particles with sizes exceeding the colloidal range, sediment quickly. According to Stoke's law given in the Equation 1, the settling velocity of spherical particles can be calculated in a fluid medium. The particle size of the oxide particles in the aqueous media should be smaller than few microns to reach required settling velocity for stabilization of the powders. As a rule of thumb, particle size smaller than 1 μm can suspend in water thus commonly preferred for colloidal stability.

$$v = \frac{(\rho_s - \rho_m) g a^2}{18\eta} \qquad \text{Eq. 1 [28]}$$

Where v is the velocity of particle, g is the gravitational acceleration, η is the viscosity of medium, a is the particle diameter, and $\rho_s \; and \; \rho_m$ are the density of solid particles and the fluid medium, respectively.

The terms of primary particle, agglomerate, and aggregate are commonly used in in this study, so they are defined in order to prevent any confusion. The primary particles are the discrete smallest solid units in different geometrical forms such as spherical, rod-like, or bulk form. It is almost impossible to break the primary particles into smaller units unless ultrahigh energy is applied.

The agglomerates are loose cluster of primary particles which are combined by weak forces or bridging of solid and liquid. Therefore, large agglomerates can be broken down into primary particles, or into smaller agglomerates by mild mechanical or ultrasonic treatments or using dispersants [29].

On the other hand, when the primary particles are clustered via chemical bonds, aggregates are developed. It is tough to break down the aggregates into primary particle size or into smaller aggregates. In such cases, high energy mechanical or ultrasonic treatments are required. In order to obtain high colloidal stability, first the particles with desired size have to be obtained. Generally, if the size of the aggregated and agglomerated particles is above few microns, they should be broken into smaller units to prevent their sedimentation due to gravitational forces. The agglomerated particles then can be dispersed considering the effective interparticle interactions.

Many advanced ceramic formation techniques such as slip casting, tape casting, electrospinning, robocasting require the dispersion and stabilization of ceramic powders in liquid media [30]. The main drawback of the colloid size particles is their tendency to form agglomerates because of the attractive interparticle interactions in liquid media. The agglomerated particles in the suspensions can lead to inhomogeneities, low packing density, higher pore distribution, and non-uniform properties in the final structure. Therefore, optimization of the interparticle forces between the colloid particles and the medium takes essential place, to obtain high quality suspensions, thus high-quality end products.

2.2. Interparticle Forces

The main interparticle forces which play an essential role in the stabilization of the oxide powder suspensions are van der Waals (V_{vdW}), electrostatic (V_{elect}), and polymer-induced ($V_{polymer\text{-}induced}$), steric and electrosteric forces. The colloidal stability of the particles is described by the total interparticle potential, V_{tot} shown in the Equation 2 [31].

$$V_{tot} = V_{vdw} + V_{elect} + V_{polymer-induced} \quad \text{Eq. 2}$$

2.2.1. Van der Waals Forces

Origin of the van der Waals force is the electromagnetic forces, particularly the dipole interactions of the particles in fluid media, which is always attractive for identical bodies. Van der Waals forces are relatively long-range forces compared to other interparticle forces since the potential energy of the particles reduced the sixth power of the distance between the molecules [32]. Hamaker stated that the van der Waals energy can be simply represented as in Equation 3 [33]. In this equation, *A* is the Hamaker constant, and *D* is the separation distance between the particles. The Hamaker constant is a material property, and it is related to the dielectric property of the atoms in medium.

$$V_{vdW} = -\frac{A}{12\pi D} \quad \text{Eq. 3}$$

As shown in the Equation 3, the strength of van der Waals energy rely upon the Hamaker constant and the geometry of the bodies while, the Hamaker constant relies on material properties like dielectric and optical properties of particles and the intervening medium [34].

To overcome the relatively long-range attractive forces, the repulsive force should be introduced. Electrostatic, polymer-induced steric, and electrosteric stabilization mechanisms are mainly used for this purpose.

2.2.2. Electrostatic Forces

Stoichiometric crystals with defect-free structure, like zinc-blend type diamond, keep their surface neutrality in the liquid systems. On the other hand, oxide particles get charged in a liquid media, particularly in a polar liquid. The main mechanisms of surface charge in liquid medium are the ionization or dissociation of the oxide surface

in solution, adsorption of ions onto the oxide surface, and ion exchange with the solution.

Once surface is charged, counterions (oppositely charged ions) are collected at the surface of the particles since opposite charges attract each other. Density of ions varies near the surface of the charged particle, so each particle is surrounded by an electrical double layer (EDL). The double-layer consists of Stern and diffuse layer [35]. The Stern layer is formed by chemically adsorbing charge onto the surface, and excess opposite charges in the solution form the diffuse layer. The diffuse and Stern layers are shown in Figure 2.1.

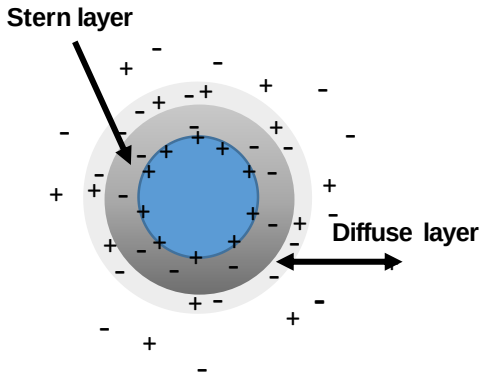

Figure 2.1. Schematic for double layer formation around particle

The thickness of the EDL is an essential parameter for electrostatic stabilization of the particles, and the thickness is equal to the inverse of the Debye parameter, κ^{-1} :

$$\kappa^{-1} = \frac{\varepsilon\varepsilon_0 kT}{e^2 \sum_1 n_i z_i^2} \qquad \text{Eq. 4 [33]}$$

In this equation e is the charge of an electron, n_i is the concentration of the ions with a valency of z_i, ε and ε_0 are the dielectric constants of medium and permittivity of vacuum, respectively.

The electrostatic interaction of two semi squares energy is described by Equation 5,

$$V_{elect.} = 64kTn_0\kappa^{-1}\gamma_0^2 \exp(-\kappa D) \qquad \text{Eq. 5 [33]}$$

In Equation 5, γ_0 represents the constant ranging between 0 and 1 as a function of the surface charge of the particles and n_0 is the concentration of the ions in the particle. It is almost impossible to measure the surface charge of the particles because of the thin liquid layer on the surface. The potential at the shear plane, located outside the Stern layer is measured rather than surface potential by electrophoretic mobility,is called zeta potential. The zeta potential of particles is calculated by Huckel approximation as given in Equation 6 [34].

$$\zeta = \frac{4\pi U}{\varepsilon} \qquad \text{Eq. 6}$$

In this equation, ζ is the zeta potential, U is the electrophoretic mobility of the particles which is measured and ε is the dielectric constant of the medium. Then, the electrostatic repulsion potential can be simplified as in Equation 7.

$$V_{elect.} = 2\pi\varepsilon a\zeta^2 \exp(-\kappa D) \qquad \text{Eq. 7}$$

As a rule of thumb, it is known that zeta potential values higher than ±30 mV, leads to stable suspensions [36–40].

2.2.3. Polymer Induced Forces

Polymer-induced forces provide alternative routes for stabilization of colloidal suspensions when enough repulsive force cannot be introduced to the colloid systems electrostatically. Steric and electrosteric stabilization techniques are the widely used under this stabilization techniques.

2.2.3.1. Steric Force

Adsorption of molecules (polymers surfactants or other organic molecules) onto particle surfaces in liquid medium is required to introduce the steric stabilization.. Two

effects play role in the steric stabilization: ΔG_{mix} represent the osmotic repulsion, and $\Delta G_{elastic}$ is stemmed from entropic decrease. The overall steric effect is the sum of ΔG_{mix} and $\Delta G_{elastic}$ [41]**.** Good coverage and relatively optimum concentration of polymers adsorbed on the particle surface is required. Also, the thickness of the adsorbed layer should be high enough to provide repulsion. Besides all these, the polymer should have good affinity with the solvent and powder, which polymer can stretch into solution for steric repulsion. If these criteria are not met, the particles can flocculate due to adsorption of additives on particle, thus lead to bridging flocculation [42].

When the adsorbed surface distance is between the L and 2L (L< h <2L), the elastic effect is negligible. L is the adsorbed layer thickness and h is the separation distance. Therefore, mixing energy determines the steric energy. At small distances h<L, both mixing and elastic effect are important. The total energy is equal, to sum up, the two effects. Figure 2.2 gives the schematic representation of steric stabilization mechanism.

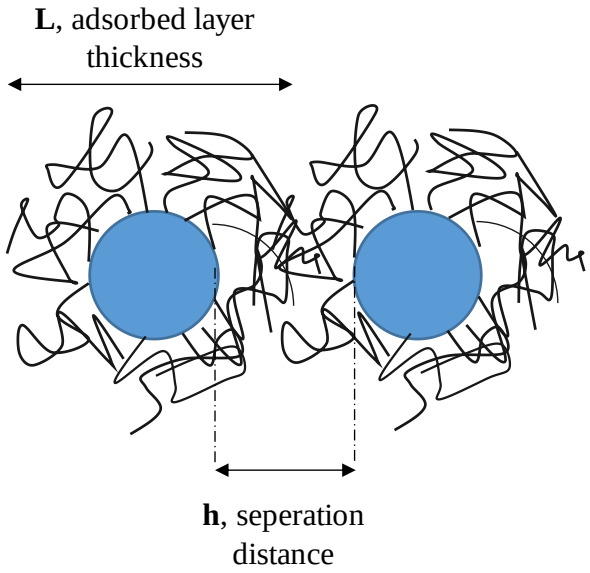

Figure 2.2. Schematic representation of the steric stabilization

Different polymer kinds are used for steric stabilization. Example include homopolymers, di-block polymers, comb-like polymers, and surfactants. Also, polyelectrolytes are another organic group, but the stabilization mechanism is slightly different from the others. Therefore, the next part stabilization mechanism of the polyelectrolytes is investigated.

2.2.3.2. Electrosteric Forces

Electrosteric stabilization is composed of a combination of both electrostatic (double layer) and steric repulsion. Ionized polyelectrolytes in solvents preferentially adsorp on the particle surface and their organic tales introduce steric forces. Therefore, combination of both electrostatic and steric stabilization mechanisms are effective in electro-steric stabilization [43]. A separation distance of the particles determines the effectiveness of the electrosteric repulsion. The electrostatic repulsion becomes more dominant at large separation distances when compared to the steric repulsion. When particles are at smaller separation, the steric repulsion has much more active on the stabilization of particles.

The ions introduced into the solvent as a result of dissociation of polyelectrolytes in liquid media should also be taken into consideration. They may affect the particle surface and/or medium properties by changing pH or ionic strength of the medium, therefore their concentration should be optimized.

When charges of particle surface and polymer are opposite, highly effective adsorption of polymer is expected due to electrostatic interactions. Therefore, the surface charge of the particles affects the adsorption quality of the polymers. In addition to the particle surface charge, solution properties (pH and ionic strength) affect the conformation and adsorption quality of the polymers [44]**.** For instance, Cesarano and Aksoy showed that dissociation of the poly (methacrylic acid) (PMMA) polyelectrolytes in the aqueous media can be altered by changing pH and NaCl concentrations. When the pH of the solution is higher than 8.5, the fraction of the

dissociation of the functional group was almost 1. Besides, the addition of the indifferent electrolyte, NaCI in their study increased the dissociation fraction at lower pH values [45]. Also, the quantity of the polyelectrolytes be used is critical because small amount of polymers may lead to the agglomeration of particles due to the neutralization of particle surface charges with ions dissociated in solution. Electrosteric stabilization mechanism is illustrated in Figure 2.3.

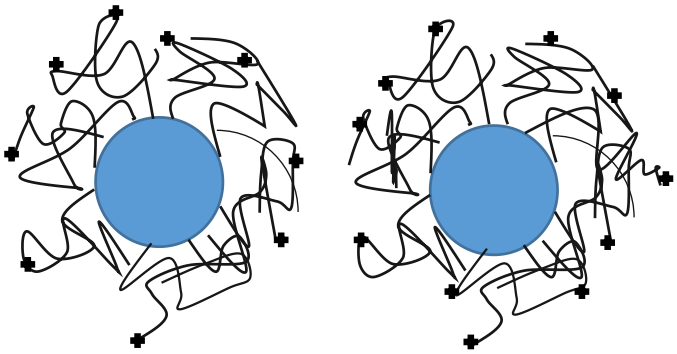

Figure 2.3. Schematic representation of the electrosteric stabilization. blue circles represent the particle, adsorbed polymer is the black line and ions are represented by +.

2.3. DLVO Theory

The DLVO (Derjaguin, Landau, Vervey, and Overbeek) theory is proposed to predict the stability of suspensions based on the balance between the attractive and repulsive forces present between the particles [46]. By sum up those forces given in Equations 3 and 5, the total energy of the system can be calculated as shown in Equation 8 [26]. Figure 2.4 shows attraction, repulsive, and net overall energy estimated by DLVO theory. The energy barrier in Figure 2.4 represents the energy amount required for agglomeration of the particles, which is related to Hamaker constant, surface potential, ionic strength, and shape of the particles according to Equation 8. Small energy barriers can be surpassed simply by the thermal vibration energy of particles. Therefore, a high energy barrier is required to obtain long term stabilization. The energy barrier can be decreasing by the amount of electrostatic repulsion with

increasing the ionic strength or by adjusting suspension pH towards the point of zero charge.

$$V_{tot} = 64kTn_0\kappa^{-1}\gamma_0^2 \exp(-\kappa D) - \frac{A}{12\pi L} \qquad \text{Eq.8}$$

The magnitude and sign of the surface potential of particles depend on the pH of the medium since hydrogen and hydroxyl ions are potential determining ions and change the surface charge at pH value. The net surface charge of the particles becomes zero at a specific pH, known as isoelectric point. Around this pH, the attractive vdW forces, dominate the system. Therefore, for electrostatic stability, suspension pH should be away from the isoelectric point in other words particles can be stabilized by adjusting the suspension pH. As depicted from Equation 4, ionic strength of the solution should be taken into consideration since the double layer thickness is inversely related to the ionic concentration in solution. When the indifferent electrolyte concentration increases, double layer thickness (κ^{-1}) decreases, which leads to a decrease in repulsive energy. To obtain colloidal stability, the repulsive force between the particles should be high enough to overcome attractive vdW interactions. Hamaker constant of the suspensions related to the attractive vdW energy, shown in Equation 3. Calculating or measuring the Hamaker constant in different systems (material and solvent) is complicated. As a general rule, the dielectric constant of the solvent is directly related. For instance, Somasundaran reported that Hamaker constant of the alumina suspensions decreases in low dielectric constant mediums such as cyclohexane or chloroform [47]. However, poor stability of alumina particles was observed in the low dielectric constant solvents. It can be explained oxide materials can introduce significant amount of the surface charge that provide electrostatic repulsion in polar mediums. Also, the minimum thickness of the adsorbed layer could be determined by value of Hamaker constant to produce colloidal stable particles [48].

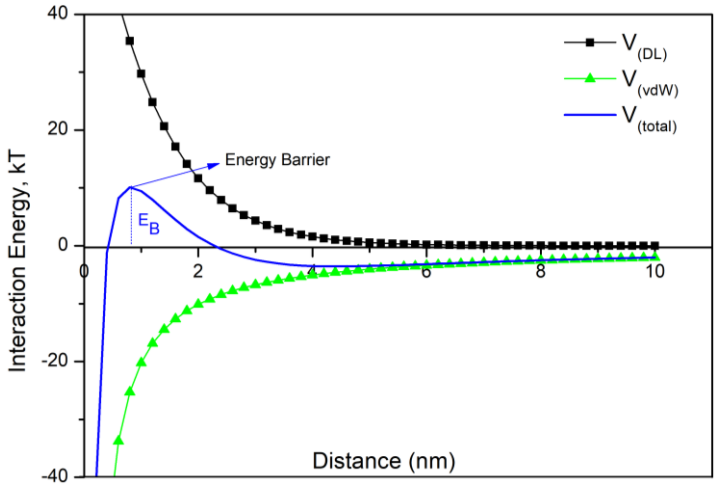

Figure 2.4. Hypothetical interaction energy (kT) versus distance (nm) curves of DLVO interactions. The attractive van der Waals attractive energy (V_{vdW}), and Double-layer repulsion energy (V_{DL}) form net total energy (V_{total})

2.4. Zeolite: Fundamental Concepts

Zeolites are crystalline aluminosilicates, which are built up from corner-sharing SiO_4 and AlO_4 tetrahedra with micro- or nano-porous structures [49]. SiO_4 and AlO_4 tetrahedrons formed zeolite structures that lead to electrical charge imbalance. Si and Al cations generally exist in +4 and +3 oxidation states in nature, respectively [50]. During the formation of tetrahedra or tetrahedrons, Si ions are substituted with Al ions, which create electrically missing electron(s). Each AlO_4 tetrahedron exhibits a net negative charge, and an extra-framework cation balances the negative charge sites. Alkaline or alkaline metals are generally found on the external surface of zeolites to electrically balance the structure; in some cases, protons, rare-earth ions or organic species may locate in the structure [50]. The structural formula of the zeolites can be written as:

$$M_nO \cdot Al_2O_3 \cdot ySiO_2 \cdot wH_2O \qquad \text{Eq. 9}$$

In Equation 9, the notation *M* represents the extra framework cations with a valence of *n* in the zeolite structure, and the H_2O stands for the water molecules in the channels or in the interconnected voids. The water may be removed reversibly, in general, by

the application of heat. This process leaves the crystalline host structure intact, permeated by the micropores and voids, up to 50% of the crystals by volume.

The classification of zeolites was required because various zeolite types have been introduced. Structure Commission of the International Zeolite Association (IZA) introduced more than 200 zeolite structures until 2017 [51]. Zeolites used to be classified as Si/Al ratios, as low, intermediate, and high Si/Al zeolites. Then, pore diameters of zeolites have used as a classification system. Three letter code was introduced to define framework type, which was confirmed by the Structure Commission of the International Zeolite Association. Today, zeolite structures are classified by the three-letter code. For instance, the LTA code illustrates Linde zeolite A or ZSM-5 code identifies the Zeolite Socony Mobil–5 zeolite [52].

Zeolites have been used in large quantities in a variety of commercial applications. According to a market research report, it expected that synthetic zeolite projects grow from 5.2 billion $ in 2018 to 5.9 billion $ by 2023 [53]. Zeolites are utilized as catalyst, e.g. in the petrochemical industry and green chemistry for the conversion of biogas to biomass and water treatment, as molecular sieves for separating and sorting molecules, as well as other application areas, shown in Figure 2.5 [54].

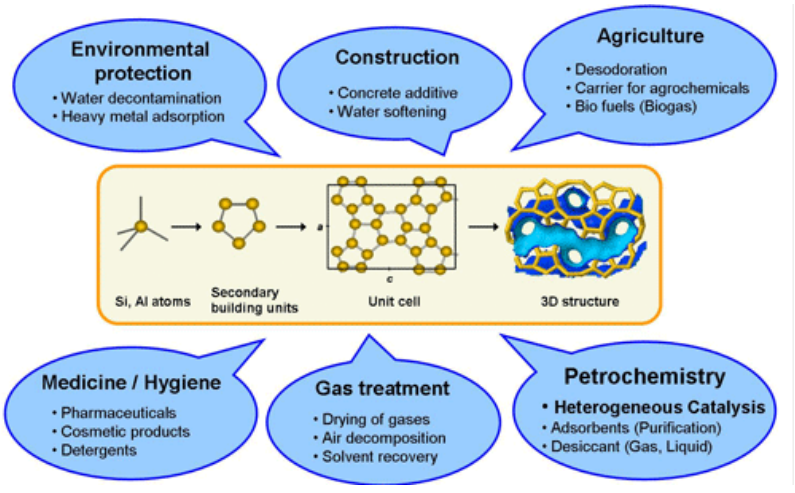

Figure 2.5. The broad field of zeolite applications [54]

2.4.1. Characteristics of Zeolites and Their Suspensions

Zeolites mainly have the tetrahedral structure, TO_4, T indicates Al or Si atom. The cornering sharing TO_4 creates a three-dimensional structure, and the framework structures of zeolites are defined as pore openings and dimensions, which shown a variety with different zeolite structures [55].

The Si/Al ratio is the most critical parameter for applications since the ratio affects the surface property of zeolites, amount and distribution of negative charge densities, pore structure, and differences in the position of SiO_4, AlO_4 molecules and cations at the extra-framework [56]. Therefore, zeolites attracted a great deal of attention among the researchers and scientists due to their adjustable macro- and nano-sized pore dimensions, ion-exchange properties, acidity in the structure, hydrophilicity and high thermal stability via altering Si/Al ratio and structure [57–59].

The colloidal stability of the zeolites mainly depends on their Si/Al ratio. For instance, high Si/Al ratio zeolites are used in an acidic environment since they can protect their Si/Al ratio without dissolution [60,61]. In addition to that, the total acidity of the zeolite increases when the Si/Al ratio reduces since acidity in the zeolite framework is related to the substitution of aluminum atoms, which leads to negative charge [62]. Kawai and Tsutsumi evaluated the hydrophilic-hydrophobic character of zeolites having different Si/Al ratios by measurements of immersion heats of the zeolites, in water. When the Si/Al ratio of the zeolite is higher than 30, the water contact angle on the surface reached the infinity, indicating the hydrophobic surface. On the other hand, if the Si/Al ratio of zeolite is lower than 30, the water contact angle on the zeolite surface becomes zero, i.e., the zeolites considered as hydrophilic [63].
Consequentially, the Si/Al ratio of zeolites influences the dispersion behavior in the liquid media due to its effect on the surface charge, acidity, and hydrophilicity/hydrophobicity.

2.4.2. Selected Zeolite Framework

Selected Zeolite Framework: Zeolite A or LTA

Despite more than 200 zeolites introduced in literature, some of them have been used in industrial applications such as Linde A (LTA), sodalite (SOD), faujasite (FAU) [64]. Here, the characteristic of LTA zeolite (Zeolite A) will be discussed in.

The general representation of NaA zeolite, i.e. Linde A type zeolite (LTA) [65], is given in Equation 10.

$$|Na_{12}H_2O_{27}|_8[\,Al_{12}Si_{12}O_{48}]_8 \qquad \text{Eq.10}$$

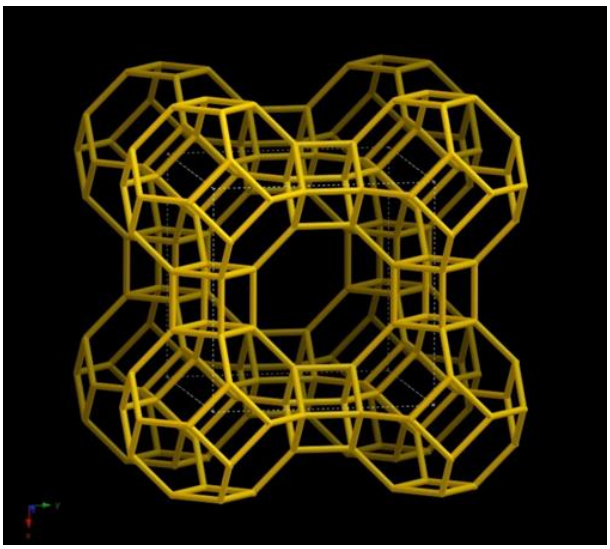

Figure 2.6. LTA zeolite viewed along [100] retrieved from IZA [65]

Corner structure of LTA zeolite forms by β-cage and α-cage is in the center of the structure shown in the Figure 2.6. The sodium ion in the zeolite structure can exchange with other ions, for instance, with potassium, calcium, or lithium cations. When different cations were used to obtain charge balance, pore dimensions shows the difference based on the cation type [66].

It is not possible to find LTA zeolite (Zeolite A) powders in nature; therefore, LTA zeolites have been artificially synthesized by hydrothermal, microwave-assisted

methods and so on. The Si/Al ratio of synthesized LTA zeolites was commonly ~1, but a higher Si/Al ratio of LTA zeolites (12-40) has been found [67,68].

LTA zeolites have mainly been studied and applied for various applications. Figure 2.7 indicates increasing trends in the number of publications which mentioned about LTA zeolite in years [6]. LTA zeolites are extensively used as zeolite membranes for the adsorption/separation of light gases such as methane or for biodiesel production from transesterification of trifolin [69,70].

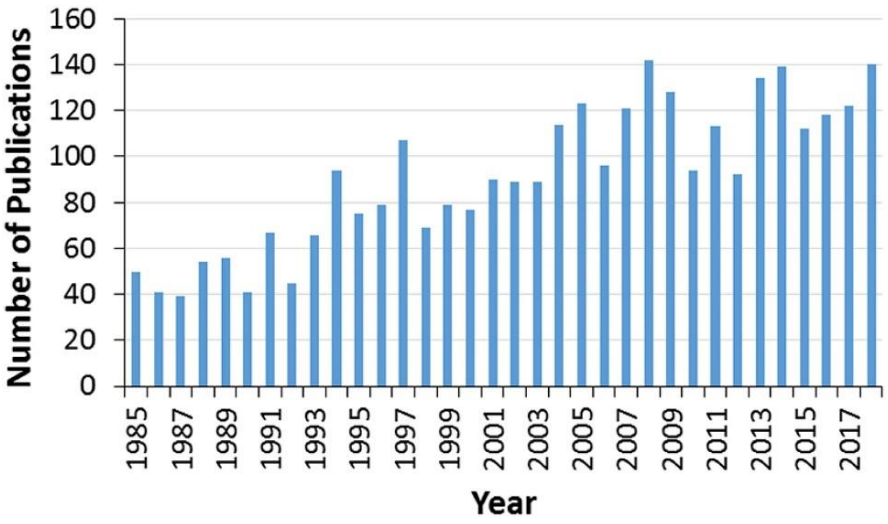

Figure 2.7. Publications mentioning "Zeolite LTA" [6]

2.4.3. Fabrication of Zeolite Structures via Colloidal Processing and Importance of the Stabilization of Zeolite Suspensions

In recent years, several processing routes, such as electrophoretic deposition, electrospinning, 3D-printing or mainly robocasting, and slip-casting are introduced to the literature for preparation of the nano-sized ceramic structures and complex ceramic shapes. These production methods have been proposed to fabricate fast and highly reproducible preparation of defect-free, good quality, and complex shape zeolite structures. These methods commonly start with dispersed zeolite powders in the

polymer containing suspensions. Therefore, in order to obtain high quality end product, the dispersion quality of the zeolite powders in aqueous and non-aqueous media is of great importance.

Depending on the processing route of interest and the required processing conditions, different solvents may be used. Here, the use of these novel processing routes for zeolites is discussed in terms of their dispersion qualities in three groups of medium: in aqueous media, in non-aqueous media, and in mixed systems.

2.4.3.1. Preparation of Zeolite Powder Suspensions in Aqueous Media

There are only a few studies in literature in which the stability of zeolite structures in aqueous media is discussed.

One of these studies belong to Akhtar and Bergström [17]. They reported the production of 13X zeolite monoliths by slip-casting of the zeolite powders using aqueous zeolite suspensions. The zeta potential of the 13X powders in deionized water is reported -4.7 mV and the suspensions were stabilized by adjusting the pH.

In another study, the MFI zeolite templated monoliths were formed by casting of the zeolite suspension on a template, then the thermal treatment process was applied. HCI was added into zeolite suspensions to stabilize the MFI powders. Although the pH range of the MFI zeolite suitable for the pH adjustment is limited due to dissolution/leaching behavior, they could still impart enough zeta potential without changing the zeolite structure in pH value above 11 [71].

In another study, zeolite monoliths were produced via Robo-casting (3D printing) of 13X and 5A zeolites in deionized water in order to be used in the removal of CO_2 gases [9]. 13X and 5A zeolite powders could be stabilized in deionized water, without use of any additives for stabilization due to their high surface charge.

SAPO-34 zeolite honeycomb-like monoliths were formed by the Direct Ink writing method, (3D printing) [72]. There was no detailed information about the stabilization

of the powders in deionized water, so the powders are considered stable in deionized water, Methylcellulose, Poly (acrylic acid) and graphene mixture.
5A zeolite monolith shapes were produced to use in the adsorption of CO_2 gases [73]. The particles were dispersed via extrusion on 5A zeolite powders in this study.

2.4.3.2. Preparation of Zeolite Powder Suspensions in the Non-Aqueous Media

The zeolite structures obtained by using non-aqueous suspensions are summarized in this section.
Matsunaga *et al.* reported the production of tubular zeolite membranes with inner surfaces coated with zeolite L powders via electrophoretic deposition (EPD) [74,75]. Before the EPD process, zeolite powders were dispersed in ethanol by ultrasonic treatment and magnetic stirrer. Then, agglomerated particles in the suspension were separated by sedimentation classification, and only supernatant of the suspension was collected for EPD or slip casting even though ethanol is used as a solvent.
In another study, Di *et al.* reported the fabrication of the zeolite hollow fibers with a silicalite1 nanoparticles without any stabilization treatment in ethanol media via coaxial electrospinning to increase the diffusion rate in the pore of silicalite-1 [76]. This study investigated the electrospinning of the zeolite Y powders in a polymer containing ethanol solvent [77]. Dispersion of the PVP containing zeolite suspensions was reached with sonication of the suspensions in a bath for almost eight hours to obtain smooth fibers. Higher solid loadings of zeolite powders led to the deagglomeration of zeolites in ethanol media. However, the poor quality of zeolite fibers was obtained when the lower zeolite content used in the suspension. Therefore, suspension parameters, powder, polymer, and ethanol concentrations and electrospinning parameters were optimized in order to obtain smooth and continuous zeolite fibers.
Olevsky *et al*. invented a novel hybrid slip casting-electrophoretic deposition process [78]. In this method, powders must be suspended in the non-aqueous or non-aqueous/aqueous mixed medium. They used 3A and 5A zeolite powders, acetone and

n-butylamine as liquid media and as a dispersant, respectively. They noted that n-butylamine did not improve the stabilization of zeolite suspensions. Yet, they did not offer an alternative chemicals to improve the stability of powders.

Kobler *et al.* reported the production of high silica zeolite-β films by spin coating due to optical and electrical properties of zeolite- β [79]. Before the spin-coating process, agglomerated particles were sedimented at the bottom of the container filled with ethanol by centrifuge, and then smaller zeolite powders were obtained. Then, the suspension, containing three binder system were spun-coated onto Si-wafer. The dispersion quality of the zeolites in the binder containing ethanol medium has not been discussed so it could be considered as stable.

In another study, the effect of the dispersion quality of Silicalite-1 zeolite suspensions on the spun-coated zeolite film has been studied [80]. Various alcohol mediums as methanol, ethanol, propanol and butanol were used to determine the suitable suspension condition for spin coating. It was concluded that highly dense silicalite-1 films were obtained when methanol or propanol are used as a solvent, but use of ethanol lead to large empty spaces and clustered powders on the substrate.

2.4.3.3. Preparation of Zeolite Powder Suspensions in Mixed Solvents

Mixed solvent mediums have been gained importance for colloidal processing of zeolites since they enable to tune properties, such as polarity, volatility, hydrophilicity, and viscosity of the medium. In the electrospinning (ES) method for example, water-based mixed mediums, particularly alcohol and alcohol-water mixtures, are used to control the rate of evaporation and to enable the production of electrospun fibers [21,81]. For spin coating, mixed solvent mediums have been used to reach desired volatility and surface tension medium[82,83]. In addition, mixed solvent media are preferred in electrophoretic deposition to reach higher voltages and improve the adhesion performance of particles[84–87] .

Despite of the increasing interest in colloidal processing of zeolites in mixed media, there are only few studies focusing on zeolite dispersion in mixed solvents.

Production of the monolith and wire gauze packings from BEA zeolites by dip-coating was studied [88]. In this study, metallic substrates were dipped in BEA powder containing butyl acetate, deionized water, and water-based butyl acetate. Even though, Teepol was used as anionic surfactant to increase the dispersion quality of particles, particularly to obtain high solid loadings, the solids content achieved by using Teepol was lower than the suspensions without any additive. The composition of Teepol mainly consists of sodium benzenesulfonate, sodium Laureth sulfate, and alcohol ethoxylate. However, there is no better alternative was present in this study.

Zhang *et al.* produced ZSM-5 nanofibers in 50:50 wt% ethanol:water media via electrospinning process. They used high molecular weight PVP molecules as a carrier polymer to enable electrospinning. The particles could be suspended in ethanol-water media without use of any additives for stabilization [89].

Although zeolite suspensions of mixed solvents have been started to be used in zeolite production, there is no study in literature which systematically evaluates the dispersion characteristics of zeolites or discusses the stabilization mechanisms which can be used for zeolite suspensions in mixed solvent media.

In the present study, common additives or polymers used for stabilization oxide particles was selected (PAA, CTAB, SLS, PVP and PEG molecules) since zeolite suspensions using additives are very limited in literature. PAA molecule was used as anionic polymer surfactant since it has been used for stabilization of the oxide particles, such as CeO_2 and Al_2O_3 [90,91]. The electrostatic adsorption of the anionic surfactant to the negatively charged (LTA) is not favorable. Rather than electrostatic interactions, PAA molecules can be adsorbed onto oxide surfaces via chemical, physical and hydrogen bonding [92]. Liufu *et al.* reported that PAA molecules could adsorbed onto negatively charged TiO_2 particles adsorbed onto oxide surface but the adsorbed amount decreases as getting further away from isoelectric point of particles [93]. CTAB, cationic polymer, is commonly used for stabilization of silica and alumina particles [94–97]. Adsorption of CTAB is favorable due to the electrostatic interactions with the negatively charged LTA powders in ethanol:water medium. SLS molecules showed dual lyophobic-lyophilic tendency and used for dispersion of

ceramic powders, particularly in the presence of polymer [98]. To study the steric stabilization method, PEG and PVP molecules were chosen. PEG molecules are generally used as non-ionic dispersant in aqueous and non-aqueous media for ceramic particles such as Al_2O_3, TiO_2 etc. [99–101]. Although PVP is not common dispersant for ceramic materials, few examples can be found in literature [100]. Low molecular weight PVP was chosen which would be effective since high molecular weight PVP molecules was used as carrier polymer etc. for following experiments.

CHAPTER 3

MATERIALS AND METHODS

3.1. Materials

LTA type zeolite powders used in experiments were provided from Technical University of Denmark. High molecular weight (1,300,000) and low molecular weight (1,500) poly(vinylpyrrolidone) (PVP) was used as a carrier polymer and as a stabilizer and were purchased from Sigma Aldrich. HCl (purity ≥ 98%) and NaOH (purity≥ 98%) tablet, were used to adjust the pH of suspensions and were purchased from Sigma Aldric. Poly (acrylic acid) (PAA) (Sigma Aldrich, MW: 5,000), Hexadecyltrimethylammonium bromide (CTAB, MW: 364.45), Sodium lauryl sulfate (SLS), and a commercial Poly (ethylene glycol) (PEG-400, MW between 380-420, Zag Chemicals, Turkey) were used as dispersants in the zeolite suspensions. The ultrapure water with a resistivity of 18.2 MΩ and technical grade ethanol (purity ≥ 96%) were used in suspensions preparation.

3.2. Powder Preparation

A received zeolite powders were, first, examined with Dynamic Light Scattering (DLS, Beckman Coulter LS 13 320, Indianapolis, USA) and Scanning Electron Microscopy (SEM, FEI 430 NanoSEM System). Then, they were exposed to a relatively high energy process; either to ball milling or to ultrasonic treatment to break the aggregated zeolite powders. In the case of ball milling, ultrapure cylinder-shaped zirconia (ZrO_2) balls, 99.99 %, are 0.5 mm. in diameter and 4.5 mm. in height were used. The weight ratio of the liquid medium, to the powder, was 4:1 (wt.) and powder to ball ratio was 1:10 (wt.). In each set, powders were added into 50 grams of a liquid medium (ultrapure water, or ethanol) and ball milled in a 100 ml PET bottle at 50 rpm.

Although the surface area of spherical zirconia balls is higher than the cylindrical balls, a higher contact region was obtained by using the cylindrical ball. Also, it is known that the mechanism of breaking powders mainly depends on the size of impact points, so cylindrical-shaped balls were selected to break up zeolite powders [102]. For the ultrasonic treatment, suitable ultrasonic pin (sonotrode S7) was used in a liquid medium by connecting UP200 St ultrasonic lab device (Hielscher Ultrasonics GmbH, Teltow, Germany). 3 grams of powder were mixed in 20 grams of liquid medium and exposed to an ultrasonic treatment at powder ranging from 35 to 100W at 25 kHz.

Before and after the treatments, particle size and size distribution of powders were analyzed using SEM and DLS analysis.

3.3. Suspension Preparation

For suspension preparation, first ethanol and ultrapure water were mixed by 50:50 weight (wt%) ratio and shaken for 3 hours at 80 rpm by shaker (Isolab 3D orbital shaker, Turkey). Then, zeolite powders were added to the solvent mixture at a concentration of 1.5 wt%, (for sedimentation experiments) or 10 wt% (for spin coating). The suspensions were ultrasonically treated for 3 min at the powder of the 35 W for homogenization with taking cooling breaks of 15 seconds for every 1 minute in order to prevent overheating and vaporization of the solvent and to keep the solid loadings constant.

For surfactant containing suspensions, selected surfactants were firstly added ethanol-water (50:50 wt%) medium and mixed by shaker 2 hours at 80rpm. Then, zeolite powders were added into the solution. The suspension was ultrasonically treated for 3 minutes at the power of the 35W for homogenization. For the preparation of carrier polymer containing suspensions, high molecular weight PVP was added into the prepared suspensions. Then, the suspension was ultrasonically mixed for 3 minutes at the power of the 35W, and similar cooling breaks described above were followed.

Rather than ultrasonic treatment, magnetic stirrer could be used for mixing the zeolite powders in the suspensions. However, ultrasonication was preferable since it mixed the suspension in less time than magnetic stirrer mixing time.

3.4. Spin-Coating Procedure

Cleaning of the 0.5x1 cm^2 silicon (Si) wafers consists of two steps. Firstly, Si-wafers immersed in acetone for 3 minutes. Then, it was removed from the acetone and placed in ethanol for 2 minutes. Finally, the surface was dried using pressurized air at room temperature.

The zeolite films were prepared by using commercial Spin-Coater KW-4A (Chemat Technology Inc, Northridge, CA)). The 100 µl zeolite suspension, including 10 wt% zeolite powder was dropped at the center of the substrates of stationary conditions. Then, the coater was accelerated to 3000 rpm in 3 seconds and rotated at this speed for 45 seconds. The zeolite films were dried at room temperature (25˚C) and characterized with SEM.

3.5. Characterization of the LTA Zeolite Powders and Suspensions

3.5.1. Scanning Electron Microscopy

The morphology and the agglomeration state of zeolite powders were characterized by Scanning Electron Microscopy (SEM, FEI Quanta 400F Nova NanoSEM 430 SEM System, Oregon, USA). To minimize the sample charging, the powders were coated a thin layer of gold by Polaron SC 7640 Sputter Coater (Watford, UK) for 2 minutes at the setting of 1.5 V and 10 mA prior to SEM examination. SEM micrographs were also used for analysis of particle size and size distribution of zeolite powders.

Energy Dispersive X-ray Analysis Spectroscopy (EDS, JEOL 2100 F, JEOL Ltd., Tokyo, Japan) was used at 20 kV for 90 seconds for elemental analysis of the zeolite

powder. For surfactant containing suspensions, the samples were firstly dried under room temperature. Zeolite powders were rinsed with ultrapure water. Then, a trace amount of zeolite suspensions was dropped onto carbon tape and left to dry. The weight ratio of Si/Al and Na/Al ratio of each sample was measured by taking average of 2 measurements at different spots of carbon tape.

3.5.2. X-Ray Diffractometry

X-Ray Diffraction (XRD, Bruker D8 Advance diffractometer) with CuKα (λ=0.154 nm) radiations were conducted at 40 kV power and 30mA current in the 2θ range of 0-70˚ and all data were collected at a rate of 5˚/min. The XRD measurements were used to investigate the purity level of the zeolite powders.

3.5.3. Dynamic Light Scattering

Dynamic Light Scattering (DLS, Beckman Coulter LS 13 320, Indianapolis, USA) was used to determine the size distribution of zeolites. The DLS analysis was performed in (ethanol, water, or their mixtures) at room temperatures (25˚C). The results of DLS measurements were reported as an average particle size based on the scattered light intensity weighted averages. Each DLS analysis was repeated 3 times for each specimen under the same conditions, and the variations in the particle size measurements were not higher than the 2%.

3.5.4. Sedimentation Measurements of Zeolite 4A Suspensions

To measure the sedimentation rate of the zeolite powders, the settling rate of the particles was observed via the amount of powders accumulated at the bottom of 10 ml of the graduated cylinder. The zeolite suspension slowly added to the tube in order to

prevent the formation of air bubbles. All sedimentation measurements were conducted at room temperature under the same visible light.

3.5.5. Electrophoretic Measurements of Zeolite 4A Suspensions

Zeta potential measurements were investigated using a Zetasizer Nano ZS (Malvern Instruments, UK) with a 633 nm red laser at room temperature (25°C). During the zeta potential analysis of LTA zeolite powders, the zeolite powders in the ethanol, water, and ethanol-water mixtures were diluted to 0.1 wt%. Polymeric dispersants and high molecular weight PVP amounts were calculated concerning the amounts of powder and suspension, respectively. Folded capillary cell (DTS1060) with a sufficient amount of volume was used for zeta potential measurements. Malvern Instruments Dispersion technology software (Version 7.0) was used to analyze the data.

3.5.6. Fourier Transform Infrared Spectroscopy

The chemical interactions between PEG, PVP, zeolites, and solvents (ethanol and or water) were analyzed using the FTIR (Fourier-Transform Infrared Spectroscopy) Frontier spectrometer with the ATR accessory (Perkin Elmer, Waltham, USA). Spectrum 10 software was used to analyze the spectra. The FTIR data collected at the absorbance mode. LTA zeolite suspensions directly put on the ATR sensor of the FTIR instrument. Before the examinations of the spectrum, interactive baseline correction at 4000 cm^{-1} was applied.

The related spectrum were subtracted from each other to amplify the difference between the spectrum. For example, in order to analyze the interactions between the PVP molecules and LTA zeolite powder, LTA zeolite spectra were subtracted from PVP containing LTA powder in the same solvent. All FTIR analyses were conducted at room temperature (25°C) and recorded over the wavenumber range of 4000 cm^{-1} to 400 cm^{-1}.

CHAPTER 4

RESULTS AND DISCUSSION

4.1. Physical Characterization of LTA zeolite powders

The chemical, physical, and surface characteristics of the zeolite powders are mainly related to the method used for their synthesis [103]. LTA zeolite powders are generally produced via hydrothermal route due to its fast reaction kinetics, low energy consumption, scalability, and cost-effectiveness [97]. However, to obtain particles without aggregates/agglomerates is a challenge in the hydrothermal route because a relatively high temperature calcination process is required for the removal of the trapped water within the porous structure of the zeolites [104].

DLS analysis and SEM micrographs of synthesized LTA powders were shown in Figure 4. SEM micrographs, presented in Figure 4.1a, show that LTA zeolite powders were composed of sphere-like individual particles with an average particle size between 300 nm to 400 nm. However, the presence of aggregates was evident. Figure 4.1a shows the necking between the primary particles, which indicate the aggregation of the primary particles, and the size of aggregates is in the micron range. DLS analysis of the synthesized powders was presented as percentage volume of particle size distribution of the zeolite powders in Figure 4.b. The trimodal size distribution of particles was observed. Based on the SEM analysis, it can be concluded the first peak shows the primary particle size of the powders was between 300 nm to 400 nm, and aggregated/agglomerated particles are > 3 μm and >10 μm, as interfered from the second and third peaks, respectively.

A settling velocity of the zeolite powders against the particle diameter in ethanol:water (50:50 wt%) was calculated by applying the Equation 1 (Stoke's Law refinement), shown in Appendix A. Appendix A shows that particle size of zeolites

should be 300- 400 nm range to suspend these particles in the medium. Therefore, in order to be able to use all powder, the aggregates should be broken into smaller units and/or primary particles, so they can be suspended in liquid media.

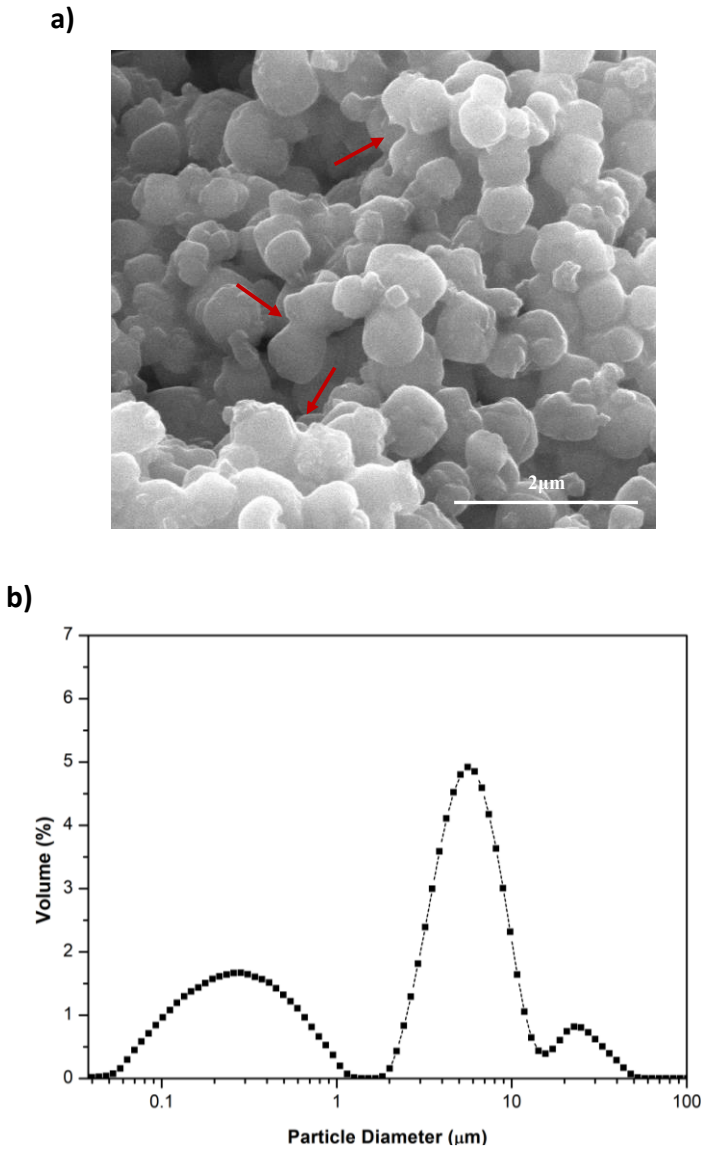

Figure 4.1. a) SEM micrographs and b) particle size distribution (by volume percentage) of as received LTA zeolite powder

4.2. Preparation of LTA zeolite Powders for Colloidal Processing

In order to be able to disperse aggregated zeolite powders in ethanol-water mediums, the particle size of the aggregate powders should be reduced. In order to break strong aggregates of zeolites, very high energy processes such as ball milling, wet milling, and ultrasonic treatment can be used. Among them, planetary ball milling was not preferred because high energy process could lead to forming pellets rather than reduce the size of the particles [105].

Wet ball milling and ultrasonic treatments are prevalent methods to break up aggregates because they are accessible and easy to handle. For this purpose, ball milling and ultrasonic treatments were employed.

The particle size measurement results of ball milled LTA zeolite powders in ultrapure water and ethanol were shown in Figures 4.2a and 4.2b, respectively. Different colors and markers in Figure 4.2 represent the various milling application time at 50 rpm milling frequency. As evident from Figure 4.2a, the second and third peaks appeared in the analysis of as-received powders (>10 μm), was disappeared but still bimodal particle size distribution was obtained even after 48 hours ball milling treatment in ultrapure water. The volume percentage of the large aggregates decreased, and particle size distribution was significantly narrowed when milling was employed for 72 hours in ultrapure water medium. However, ball milling for longer times (from 72 hours to 96 hours), led to re-agglomeration of the zeolite powders in the ultrapure water. Then, particles were re-dispersed again when 120 hours of milling was employed, as shown in Figure 4.2a. When ball milling treatments in ethanol was compared, the third peak, representing the particles larger than 10 μm, was disappeared for all treatments. Even though the volume of the aggregates decreased with milling time, the bimodal distribution of LTA zeolite powders (< 1 μm and around 2 μm) could not be eliminated even after 120 hours treatment. Therefore, it was concluded that the de-aggregation of zeolite powders was only useful in ultrapure water media. In water media, at least 72 hours were required to reach a significant number of particles, with particle size close to particle size. Before and after ball milling treatment, the similar pH of the

suspensions was 10.3 and 10.1, respectively. The pH results indicated that the chemical and surface properties of powders were preserved. Based on the particle size distribution data, ball milling at 50 rpm for 72 hours in water was chosen as optimum conditions to obtain dispersible powders.

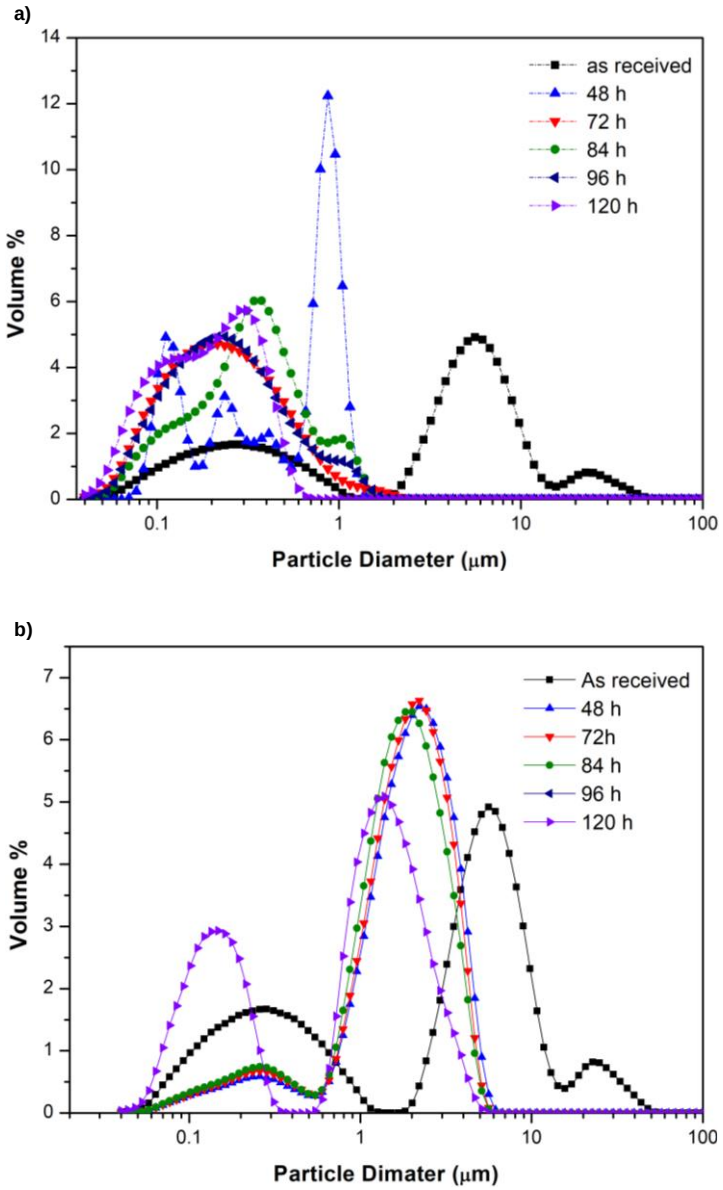

Figure 4.2. Particle size distribution of the LTA zeolite milled for 48,72,84,96 and 120 hours a) in ultrapure water b) in ethanol

In order to fasten the process, the ultrasonic treatment was employed for the de-aggregation of LTA zeolite powders. Figure 4.3 shows the particle size distribution of powders obtained after treatments at various power settings and durations. Based on the ball milling experience, water was used for ultrasonic fragmentation experiments. In addition, water media was more helpful to prevent excessive evaporation and keep the concentration constant when compared to ethanol media.

As depicted in Figure 4.3a, the large aggregates (> 10 μm, the third peak) could be eliminated even at 50 W and for 3 minutes of ultrasonic treatment. The amount of aggregates between 2 μm and 10 μm (the second peak) was significantly reduced with ultrasonic treatment at 50W for 3 minutes and eliminated with the application of higher powers (Figure 4.3a) and/or larger application times (Figure 4.3b). Even though the particle size could be reduced below 2 μm, i.e., to colloidal size range, bimodal distribution (400 nm and 1 μm) was obtained for all cases, indicating the presence of small aggregates. However, since all particles were in the colloidal range, these powders were found suitable for further studies in this thesis. The ultrasonic treatment at 70 W and 20 Hz for 5 minutes was chosen as optimum parameters for the preparation of dispersible powders.

SEM micrographs of the treated zeolite powders were obtained and shown in Figure 4.4. The SEM micrographs, after 72 hours of ball milling at 50 rpm and ultrasonic pin treatment at 70W and 20 kHz for 5 minutes, showed that the neck between the primary zeolite powders was successfully broken up without any significant change in particle shape.

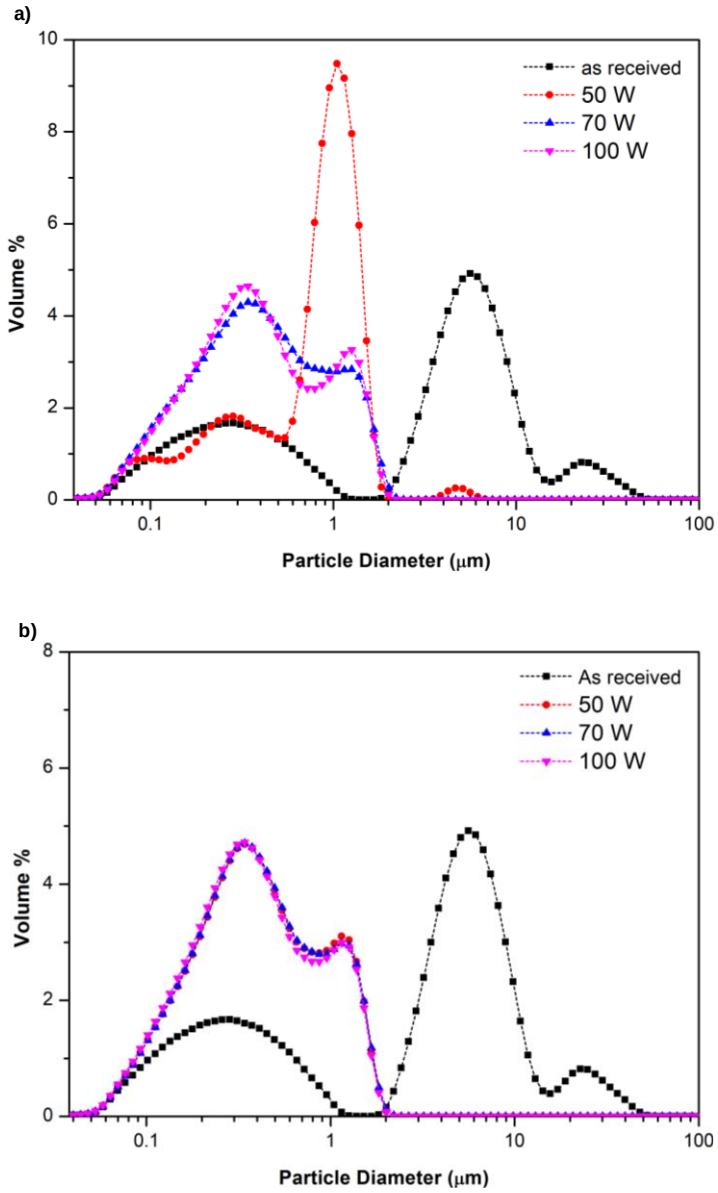

Figure 4.3. DLS particle size distribution of LTA zeolite in water as a function of ultrasonic treatment a) for 3 minutes treatment time b) for 5 minutes treatment time. 50, 70 and 100W powers were employed.

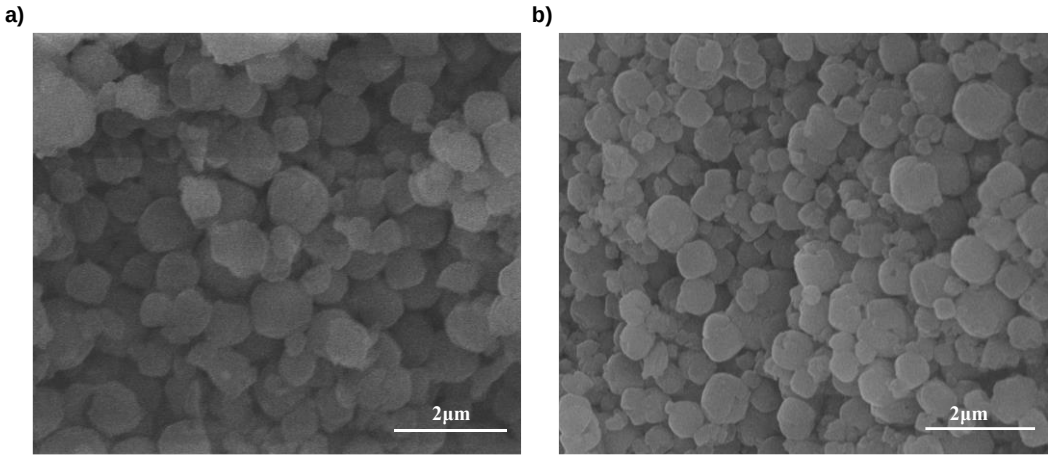

Figure 4.4. SEM micrographs of LTA powders a) powders after ball milling (72hours at 50 rpm in water); b) powders after ultrasonic treatment (5 minutes at 70 W in water)

Figure 4.5 shows the particle size distribution of powders obtained with selected optimum conditions and compares them with the distribution of as received powder. Even though smaller particles with narrower size distribution were obtained as a result of ball milling procedure, because of its rigorous process conditions, ultrasonic treatment was used for further studies in this thesis due to its practicability.

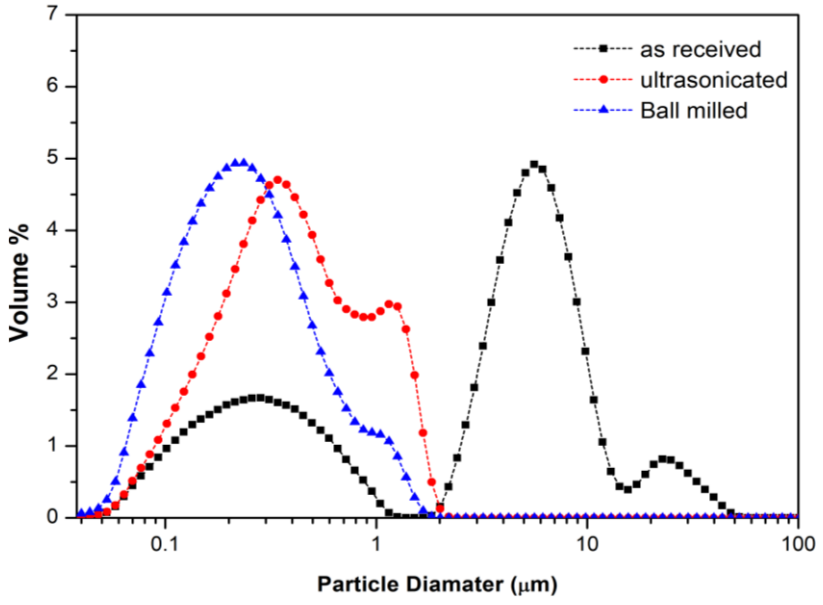

Figure 4.5. DLS Particle size distribution of as received and treated LTA powders by selected optimum process parameters. For Ball milling 72hours at 50 rpm were employed and for an ultrasonic treatment were employed 5 minutes at 70 W in water.

4.3. Stability Analysis of the LTA Zeolite in Ethanol-Water Mixed Solvents

The sedimentation characteristics of treated LTA zeolite powders were prepared to reveal the effect of ethanol amount on the dispersion quality of the powders. Figure 4.6 showed the various ethanol:water amounts (30:70, 40:60, and 50:50 wt%) against the elapsed sedimentation time. As shown in this figure, the settling velocity of the zeolite powders increased with an increasing amount of ethanol. The amount of sedimented zeolite powder at the bottom of the container remained similar in the mixed solution containing 30 % and 40 % ethanol by weight, as shown in Figure 4.6a and 4.6b; in other words, the zeolite powders suspended in the medium at least for 24 hours. Nevertheless, when the ethanol amount raised to 50 wt% shown in Figure 4.6c, a significant amount of zeolite powders was settled in 3 hours, indicating much higher sedimentation rates and potential agglomeration of primary particles.

In order to evaluate the agglomeration tendency of LTA powders in mixed solvents, the zeta potential values of powders were measured in various solvent concentrations (Table 4.1). The zeta potential value of LTA zeolite powders was as high as -49.7mV in pure ultrapure water (0:100 wt%). This value reduced to -42.4 mV, 35.4 mV, -22.8 mV in ethanol:water 30:70, 40:60, and 50:50 ethanol:water mixtures, respectively. The zeta potential of LTA zeolites in pure ethanol was -18.8 mV. Since the natural pH of samples did not change significantly, it can be concluded that the dissolution of LTA zeolites in water or ethanol was comparable and low. Therefore, the change in zeta potential can solely be explained with changes in the dielectric constant of the medium. The dielectric constant of water is 78.1, while it is 24.5 for ethanol.

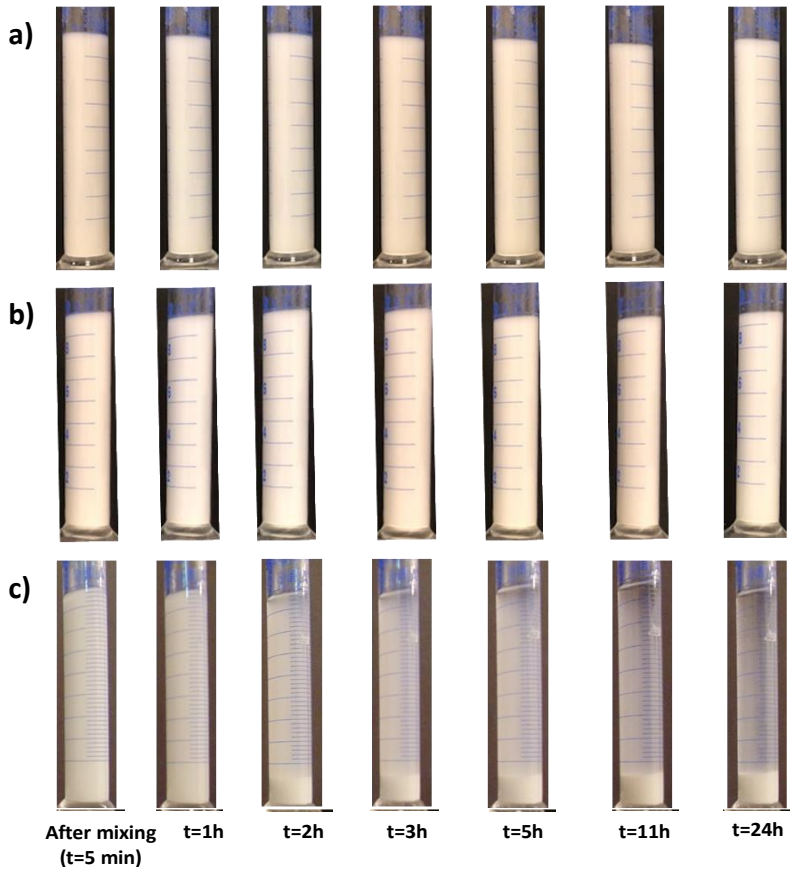

Figure 4.6. Sedimentation behavior of LTA type zeolites in ethanol:water is 30:70 in a, 40:60 in b and 50:50 in c, 1.5 wt% zeolites with respect to suspensions were used in each sample. The first image on the left-hand side is taken 5 min. after mixing LTA powders in ethanol-water mixtures.

According to Equation 6, the decrease in the dielectric constant lowered zeta potential values, thus weaken the repulsive forces given Equation 7. Besides, lower dielectric constant also leads to a faster screening of the surface potential (Equation 4). The lower zeta potential values lead to reduction in repulsive forces and may lead to faster agglomeration of powders. As mentioned in the literature review, ± 30 mV is found as a critical value to obtain stable suspensions. In line with this information, the zeta potential of LTA zeolites decreased below this limit, therefore fast sedimentation of such suspensions can be explained with inefficient repulsion between powders. Agglomerated powders get larger and larger and eventually cannot resist the gravitational forces and sediments. On the other hand, the natural surface charge, thus effective electrostatic repulsive forces, were large enough to stabilize the LTA particles

without any need for additional effort, when the ethanol concentration was 40 wt% or lower.

Table 4.1. Zeta potential measurements of LTA zeolites in various Ethanol:Water mixture and pH of the as-prepared suspensions

Sample LTA in Ethanol:Water Solution	**Zeta Potential (mV)**	**Natural pH**
0:100 wt%	*-49.7 ± 0.3*	*10.3*
30:70 wt%	*-42.4 ±0.4*	*10.3*
40:60 wt%	*-34.5 ± 0.3*	*10.4*
50:50 wt%	*-22.8 ±0.4*	*10.2*
100:0 wt%	*-18.8 ±0.6*	-

4.4. Stabilization of LTA Zeolite in Ethanol:Water (50:50 wt%) Mixture

4.4.1. Electrostatic Stabilization of LTA Zeolites in Ethanol:Water (50:50 wt%) Mixtures

In order to build enough repulsive force on LTA powder surfaces, the pH of the suspensions was adjusted using HCI and NaOH. The zeta potential values of LTA powders were presented in Table 5.2 with varying pH of the suspensions. The 10^{-2} M and 10^{-3} M of HCI or NaOH cannot impart stabilization since zeta potential values were below the critical value of ± 30 mV. On the other hand, in the presence of 10^{-1} M acid or base, zeta potential values showed two high positive values. The pH values of the suspensions were 3.32 and around 14.00, with 10^{-1} M HCI and NaOH, respectively. As shown in the table, the conductivity of the suspensions indicated high values, 8.5 mS/cm and 2.5 mS/cm with 10^{-1} M HCI and NaOH respectively. These results indicate that at those pH values, rather than suspensions became stable, and powders started to dissolve in the liquid medium with the effect of acid and base additions. Hartman *et al*. studied the dissolution characteristic of LTA zeolites and

stated that the Si/Al ratio of the zeolites affects the dissolution behavior [106]. The synthesized LTA powders showed dissolution behavior at pH values less than 4 and higher than 13. Therefore, it is not practical to stabilize the zeolite powders by changing suspension pH in ethanol:water (50:50 wt%) mixture because sufficient repulsive force cannot be introduced at the pH range where powders do not dissolve. In addition, the ions present in solution exchange with the ions in zeolite and alter the zeolite structure, thus its properties [107]. Because of the complexity of dissolution and ion-exchange property of zeolite powders, electrostatic stabilization is not suggested for LTA zeolites in ethanol:water (50:50 wt%) mixtures.

Table 4.2. Zeta potential and pH of LTA powder in Ethanol:Water (50:50 wt%) mixture containing various amount of HCI and NaOH.

Acid or Base Content	Zeta Potential (mV)	pH	Conductivity (mS/cm)
[HCI]: 10^{-1} M	*60.8 ±0.9*	*3.3*	*8.5*
[HCI]: 10^{-2} M	*2.2 ±0.9*	*7.9*	*0.8*
[HCI]: 10^{-3} M	*-15.9 ±0.9*	*9.5*	*0.7*
[NaOH]: 10^{-3} M	*-15.8 ±0.9*	*12.3*	*0.2*
[NaOH]: 10^{-2} M	*-28.3 ±0.9*	*13.4*	*0.4*
[NaOH]: 10^{-1} M	*83.1 ±0.9*	*14.0*	*2.5*

4.4.2. Steric/Electrosteric Stabilization of LTA powders in Ethanol:Water (50:50 wt%) Mixtures

For steric and electrosteric stabilization of LTA zeolite powders in ethanol:water (50:50 wt%), organic additives were used, and their effect on the sedimentation rate of zeolite powders were investigated. In this study, commonly used anionic, cationic, zwitterionic and non-ionic organic molecules, namely PAA (anionic, MW 5,000),

CTAB (cationic, MW 364.45) and SLS (zwitterionic) were chosen. These molecules are widely used for the stabilization of the oxide powders. As shown in Figure 4.7, the addition of the PAA and SLS did not improve, instead fasten the sedimentation process. This was an expected result because as known from the zeta potential measurements, the surface of LTA zeolite powders was negative. The addition of negatively charged additives did not help to stabilize LTA zeolite powders. The addition of a cationic surfactant (CTAB), on the other hand, performed better compared to the other additives and improved the stability of LTA zeolite; however, it could not completely prevent the sedimentation of LTA zeolite powders. When the pH of these suspensions was compared (Table 4.3), the CTAB addition decreased the pH slightly. Considering a very low concentration of zeolite powder and additives, the presence of these extra ions in solution might affect the stability of LTA powders.

The effect of two non-ionic low molecular weight polymers PVP (MW: 1,500) and PEG (MW: 400) on the sedimentation behavior of the LTA powders in ethanol:water (50:50 wt%) was investigated. The addition of low molecular weight PVP molecules fastens the sedimentation behavior (Fig. 4.8) while decreasing the suspension pH (Table 4.3). Since PVP molecules do not dissociate in ethanol:water mixture, the observed change in the pH might be due to the surface interactions between LTA powder and PVP molecules. The addition of the PEG molecules, on the other hand, significantly improved the stability of LTA powder (Fig. 4.8.). LTA powders were stable at least for 11 hours.

Table 4.3 EDS analysis of LTA zeolite powders (50:50 Ethanol:Water) in the presence of various additives.

Sample **LTA in Ethanol:Water (50:50 wt%)**	**Na/Al ratio**	**Si/Al ratio**
No polymer addition	*0.53*	*1.23*
Addition of PAA	*0.54*	*1.51*
Addition of CTAB	*0.61*	*1.29*
Addition of SLS	*0.42*	*1.34*
Addition of PEG	*0.53*	*1.24*
Addition of PVP	*0.55*	*1.25*

The EDS analysis of LTA zeolite powders in various additives was shown in Table 4.3. Higher Si/Al ratio of dried LTA zeolite powders was found in the polyelectrolytes added suspensions, PAA, CTAB and SLS. The ratio was slightly higher for non-ionic polymers, PEG and PVP containing suspensions than no additive LTA zeolite suspension ratio. On the other hand, Na/Al ratio showed the difference in the type of the organic additives. The ratio was considerably decreased in the presence of SLS and increased in the presence of the CTAB. The ratio was slightly increased after addition of the PAA and PVP, and it remained constant with PEG molecules. It was concluded that the ion balance of the LTA zeolite was broken down in the presence of polyelectrolytes. Therefore, the use of polyelectrolytes was not practical for the stabilization of LTA zeolite powders.

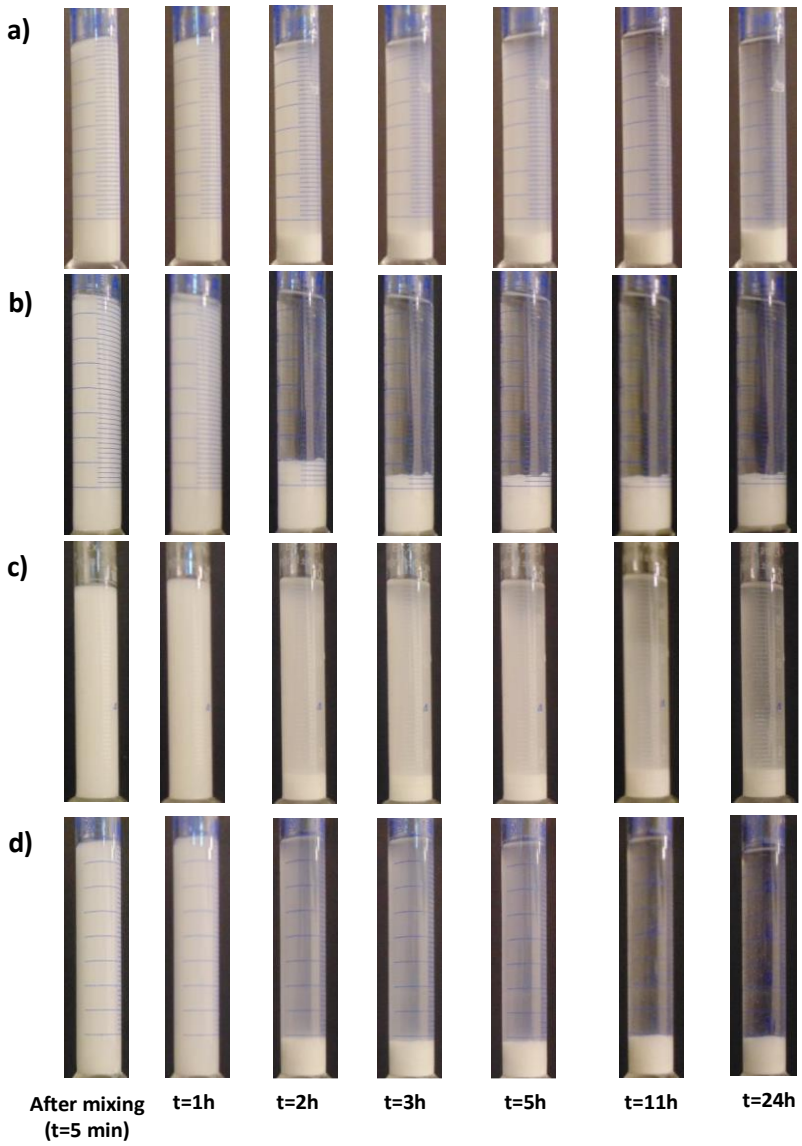

Figure 4.7. The effect of polyelectrolyte additions on the sedimentation behavior of LTA type zeolites in ethanol-water solutions in the: a) absence of additive; with addition of b) PAA; c) CTAB; and d) SLS. 1.5 wt% LTA zeolite used in ethanol-water mixture (50:50 wt%) for all samples and polymer concentration was 1 wt% of the zeolite powder.

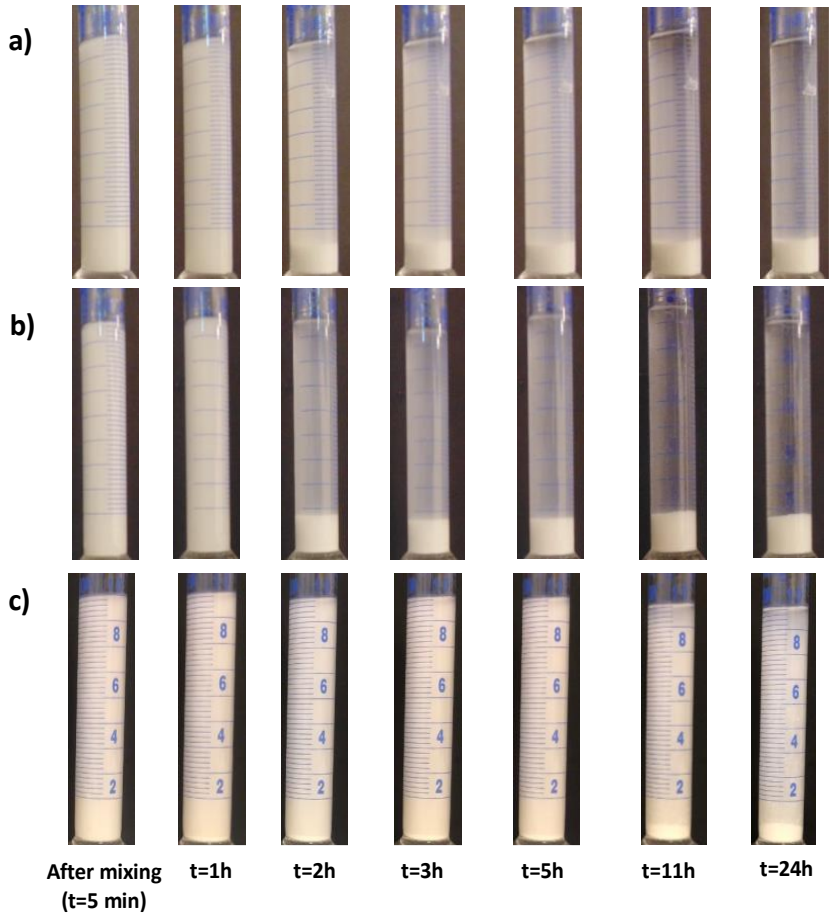

Figure 4.8. The effect of non-ionic polymers addition on the sedimentation behavior of LTA type zeolites in ethanol-water solution in the: a) absence of polymers; b)presence of low molecular weight PVP; and c) presence of PEG-400 in the 1.5 wt% LTA zeolite dispersed in ethanol-water mixture (50:50 wt%) for all samples and polymer were added as 1 wt% polymers with respect to the amount of zeolite suspensions

In order to elucidate the stabilization mechanism of PEG in LTA zeolite powders in ethanol-water mixture, the ATR-FTIR analysis and zeta potential measurements were conducted. Zeta potential value of LTA powder in the presence and absence of PEG were shown in Table 4.4. Zeta potential value of LTA powders increased from -22.8 mV to -42.9 mV by addition of PEG-400 (1 wt% with respect to LTA powder). This result explains the better stability of powders in the presence of PEG. When the pH of the suspensions was compared, there was only small change from 10.2 to 10.1 with PEG additions indicating that there is no significant change in the ion balance in the suspension.

Table 4.4. Zeta potential measurements of LTA zeolite powders and the pH of their suspensions (50:50 Ethanol:Water) in the presence of various additives.

Sample LTA in Ethanol:Water (50:50 wt%)	**Zeta potential (mV)**	**Natural pH**
No polymer addition	*-22.8 (±0.4)*	*10.2*
Addition of PEG	*-42.9 (±0.8)*	*10.1*

The ATR-FTIR analysis of the LTA powders was presented in Figure 4.9. While the red and blue lines indicate the spectra in the absence and presence of the PEG molecules LTA suspensions, respectively the green line present the difference between the red and blue lines and used to amplify the changes.

The absorbance at wavenumbers between 3500-3200 cm^{-1} was attributed to the symmetric and asymmetric stretching of hydroxyls (OH). The absorbance peak located near 2973 cm^{-1} was attributed to the C-H stretching and exhibited due to the presence of ethanol (Fig 4.9a). The absorption peak located near the 1660-1635 cm^{-1} was attributed to the stretching vibration of the functional carbonyl group (-C=O) of ethanol molecules. There was no change observed between blue and red lines near these peaks (Fig 4.9b). The wavenumbers at 1085 cm^{-1} and 1045 cm^{-1} shown in the suspension because of the C-O bond of ethanol in water (Fig 4.9b).

The peak at 1009 cm^{-1} ascribed the asymmetric stretching vibrations of bridge bonds TO_4 (T=Si or Al), observed in Figure 4.9b [108]. In the PEG-400 containing suspensions, this peak disappeared, indicating the adsorption of PEG molecules on the powder surface. Therefore, it can be concluded that PEG molecules interact with the LTA powder surface. Combined with zeta potential measurements, these interactions increased the surface charge of powder and led to better stabilized LTA suspensions.

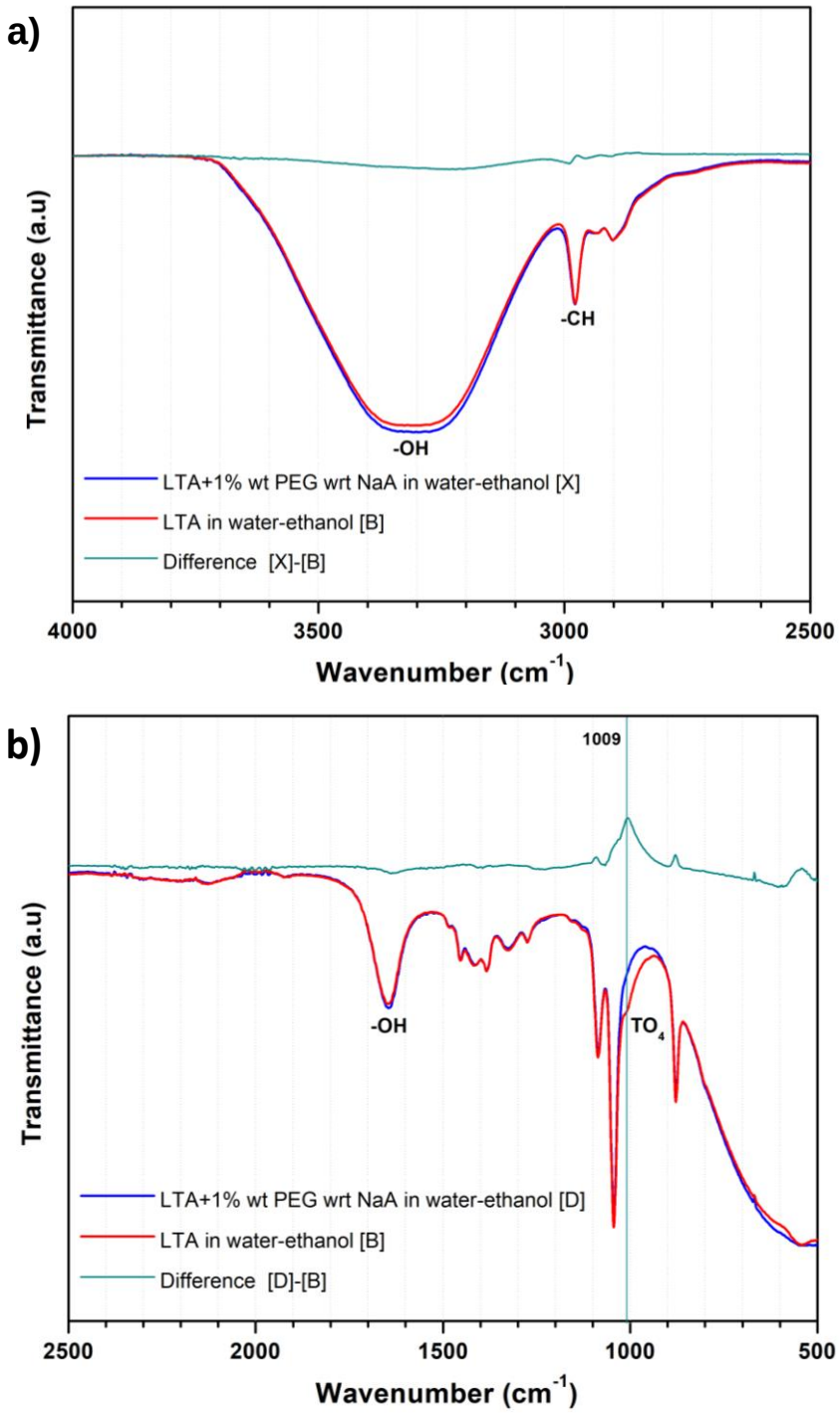

Figure 4.9. ATR-FTIR spectrum of zeolite suspensions in the absence (red spectrum) and the presence of PEG (blue spectrum). Spectrum is divided into two parts as the wavenumber range of 4000-2500 cm^{-1} (a), and 2500-500 cm^{-1} (b). Green spectra is for the difference of the blue and red spectrum.

4.5. Stability of LTA Zeolite in Ethanol:Water Mixture In the Presence of Polymer Carriers

In many processing techniques including electrospinning, tape casting, robocasting, and so on, addition of the high molecular weight polymers is required to adjust the suspension viscosity and/or used as carrier. Moreover, examples of zeolites/polymer composites exist in literature where the distribution of zeolites in high molecular weight polymer is vital [109–111]. High molecular weight PVP is one of the common polymers used for such purposes, therefore it was selected in this study.

Sedimentation behavior of the high molecular weight PVP containing LTA powder suspensions in ethanol-water mixtures, containing 30, 40 and 50 wt% ethanol was shown in Figure 4.10.

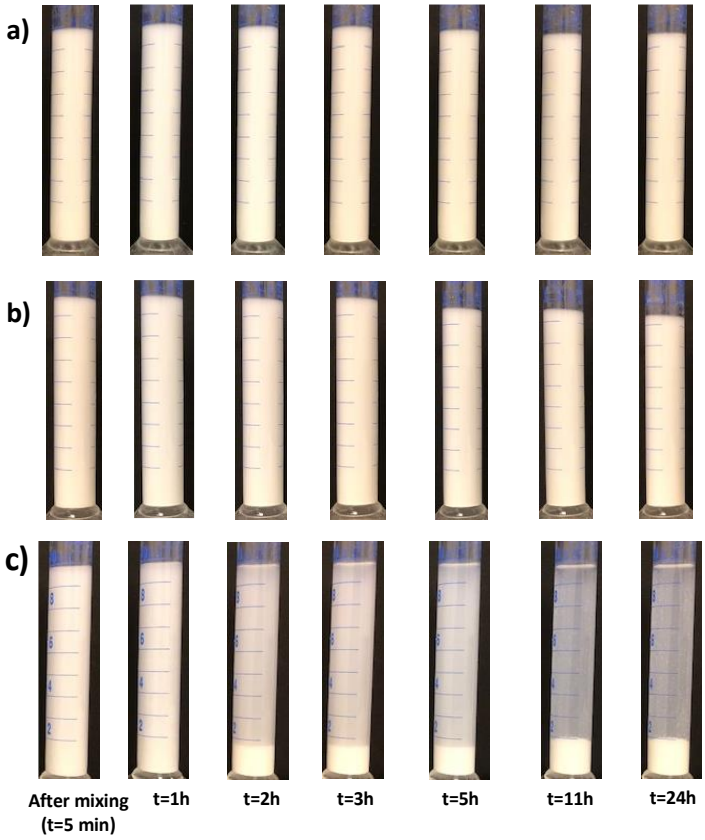

Figure 4.10. Sedimentation behavior of LTA zeolites in the presence of high molecular weight PVP in ethanol:water mixtures. 1.5 wt% zeolites with respect to suspension, 10wt% PVP with respect to zeolite powder were used. Ethanol to water ratio is a) 30:70, b) 40:60, and c) 50:50.

Even though the presence of high molecular weight PVP fasten the sedimentation rate in ethanol-water mixtures containing 50 wt% ethanol (significant sedimentation observed even after 2 hours) the stability of powders in other solutions containing 30 wt% and 40 wt% ethanol was good enough at least for 24 hours.

The zeta potential values of LTA zeolite powders were as high as -49.7mV in ultrapure water solutions (Table 4.1). This value reduced to -46.7 mV when PVP was added into solution (Table 4.5). Similar reduction was observed at all ethanol concentrations (Table 4.1 vs Table 4.5). This slight decrease in zeta potential values, from -34.5 mV to -32.6 mV for suspensions containing 40 wt% ethanol, was not enough to screen surface charges, therefore stable suspensions could be obtained with ethanol concentrations up to 40 wt%. However, in the case of suspensions with 50:50 wt% ethanol:water, already low zeta potential values decreased down to the level of -15.6 mV, which explained the accelerated sedimentation of LTA powders.

Table 4.5. Zeta potential measurements of LTA zeolites and natural pH of their suspensions in the presence of high molecular weight PVP dispersed in ethanol-water solutions with varying ethanol concentration.

Ethanol:water (wt%)	**Zeta Potential (mV)**	**Natural pH**
0: 100	*-46.7 ±0.9*	*9.8*
30: 70	*-39.4 ± 0.2*	*10.4*
40: 60	*-32.6 ± 0.3*	*10.5*
50:50	*-15.6 ± 0.3*	*9.6*
100: 0	*-4.6 ±0.2*	-

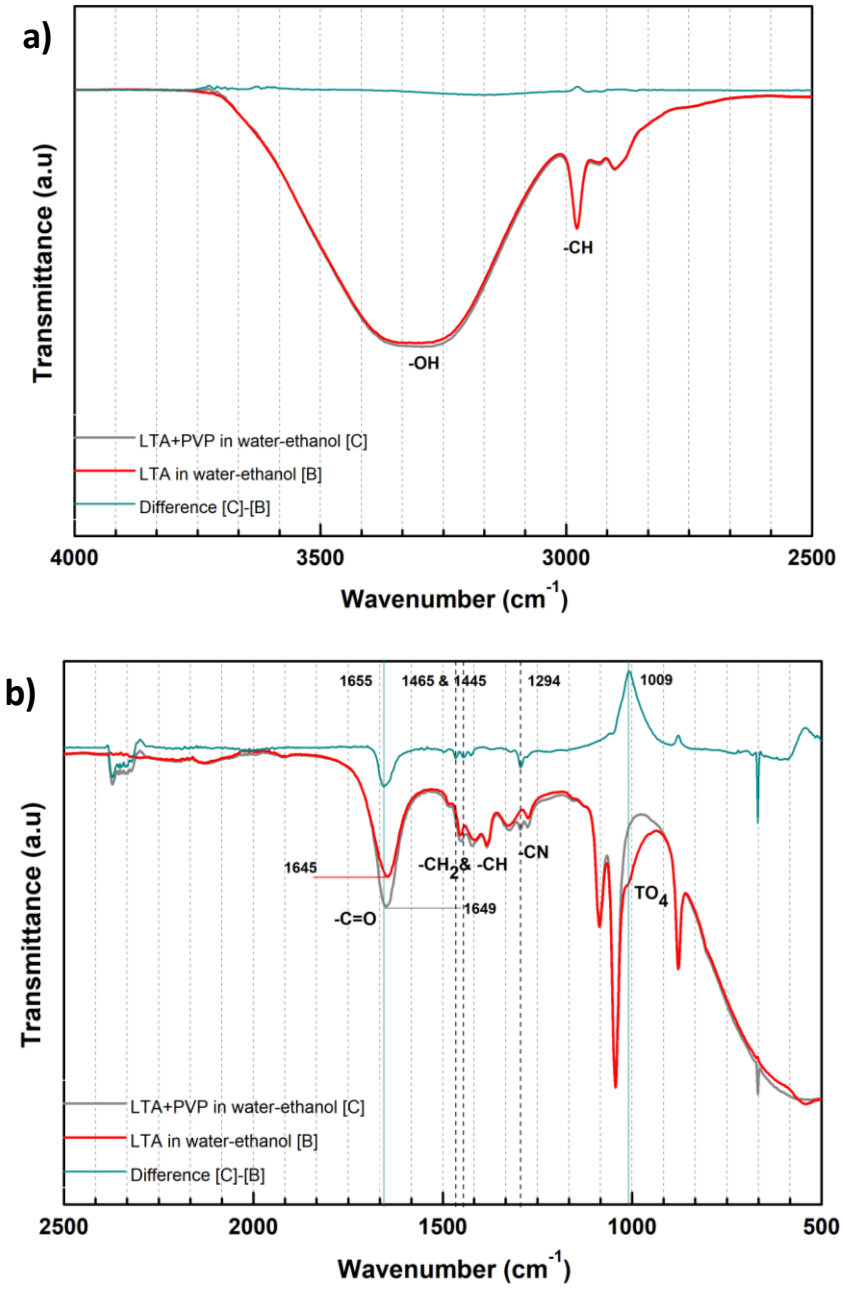

Figure 4.11. ATR-FTIR spectrum of zeolite suspensions in the absence (red spectrum) and the presence of PVP (gray spectrum). Green spectra are for the difference of the black and red spectrum. Samples contain 1.5 wt% of LTA powders with respect to suspension and 50:50 wt% of ethanol:water. The amount of PVP addition is the 10 wt% of zeolite powder. Spectrum is divided into two parts as the wavenumber range of 4000-2500 cm^{-1} (a), and 2500-500 cm^{-1} (b).

In order to investigate the level of PVP interactions with LTA powders, ATR-FTIR analysis was employed. As shown in Figure 4.11, the most obvious change was observed in difference spectra at the absorbance peak at wavenumber of 1655 cm^{-1}. This change was occurred as a result of the shift of the absorbance peak at 1649 cm^{-1} to 1645 cm^{-1}, clearly indicated the adsorption of PVP molecules on LTA zeolites through its functional –C=O groups [112]. The remaining of the peaks were typical absorbance peaks for PVP molecules in ethanol-water, shown in Appendix B.

In order to improve the stability of PVP containing LTA zeolite suspensions in ethanol:water (50:50 wt%) mixture, the effect of PEG addition was studied. As shown in Figure 4.12c, the sedimentation of LTA zeolites could be postponed for at least 5 hours after sample preparation as a result of PEG addition. When compared to LTA containing ethanol-water suspensions given in Figure 4.12a, the sedimentation rate of powders was slower even in the presence of PVP. However, it was obvious that at any condition, PVP addition destabilized LTA powders and led to agglomeration and eventually sedimentation of powders.

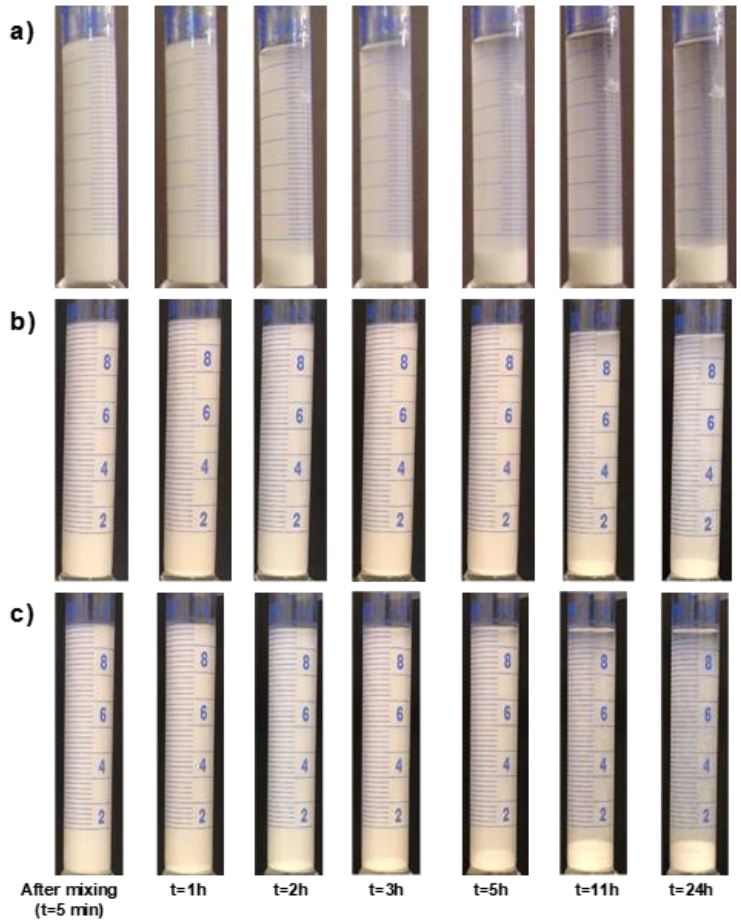

Figure 4.12. The effect of PEG addition on the sedimentation behavior of LTA type zeolites in ethanol-water solution: (a) LTA zeolites in ethanol-water solution; (b) the effect of PEG addition on the stability of LTA zeolites in ethanol water solution; and (c) the effect of PVP addition to PEG-stabilized LTA zeolites in ethanol-water solution. The ethanol to water ratio is 50:50 wt%. The amount of LTA 1.5 wt% with respect to the suspension, 1 wt% of PEG and 10 wt% PVP with respect to LTA.

Zeta potential values of the PEG and PVP containing suspensions, were present in Table 4.6. The zeta potential value of PEG-400 containing suspensions was decreased with the addition of PVP from -42.9 mV to -33.1 mV. A similar zeta potential decrease was observed with the addition of PVP molecules in LTA zeolite suspensions. However, due to the enhanced zeta potential values in the presence of the PEG molecules, -33.1 mV, were still high enough to suspend zeolite powders for 11 hours.

Table 4.6. Zeta potential of PVP-containing LTA suspensions in Ethanol:Water (50:50wt%) mixtures in the presence/absence of PEG molecules

Additives	Zeta potential (mV)	Natural pH
No additive	*-22.8 ±0.4*	*10.2*
10 wt% of PVP with respect to zeolite powder	*-15.6 ± 0.3*	*9.6*
1 wt% of PEG with respect to zeolite powder	*-42.9 ±1.5*	*10.1*
10 wt% of PVP and 1 wt% of PEG with respect to zeolite powder	*-33.1 ±0.8)*	*9.8*

In addition to the zeta potential measurements, ATR-FTIR analysis was employed in order to investigate the interactions between PEG and PVP molecules with LTA zeolites.

In the spectrum presented in the Figure 4.13, similar to Figure 4.11, the most obvious change which could be observed at difference spectra was the absorbance peak at wavenumber of 1656 cm^{-1}, occurred as a result of the shift of the absorbance peak at 1649 cm^{-1} to 1645 cm^{-1}. This shift indicated the adsorption of PVP molecules on LTA zeolites through its functional –C=O groups.

The exhibited wavenumbers from 1465 and 1445 cm^{-1} were related to the vibrational bands of -CH_2 and -CH. The wavenumber 1293 cm^{-1} is attributed to the -CN vibrations of PVP molecules shown in Figure 4.13b [113]. Those peaks are similar to the ones Figure 4.11b which was originated from PVP presence in the ethanol-water mixture.

Similar to the spectrum presented in Figure 4.9, PEG molecules interact with LTA surface and leads to disappearance of the absorbance peak at the wavenumber of 1009 cm^{-1} as shown in Figure 4.13. As a result, it was concluded that both PEG and PVP molecules interact with LTA surface without any specific interactions between PEG and PVP molecules that can be detected by ATR-FTIR analysis. Therefore, the

positive effect of the PEG addition on stabilization was observed even in the presence of the high molecular weight PVP molecules.

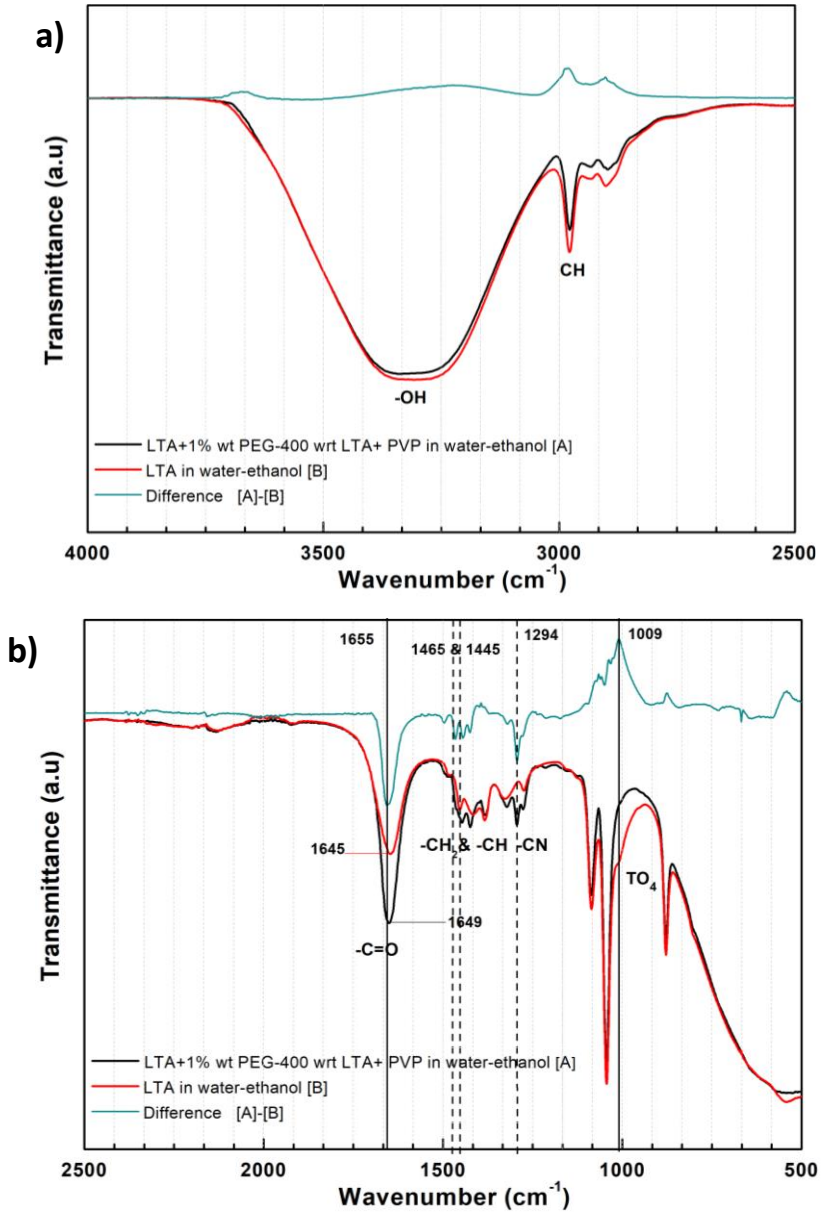

Figure 4.13. In situ ATR-FTIR analysis show the effect of PEG and PVP addition to the LTA in ethanol-water solution. The amount of LTA 1.5 wt% with respect to the suspension, 1 wt% of PEG and 10 wt% PVP with respect to LTA. Red spectra is for the LTA in ethanol water, blue spectra is for LTA in ethanol water in the presence of PEG, black spectra is for the LTA in ethanol water in the presence of PEG and PVP and the green spectra is the difference of the black and red spectrum. Spectrum are divided into two parts as the wavenumber range of 4000-2500 cm^{-1} (a-c), and 2500-500 cm^{-1} (b-d).

4.6. Case Study: The Influence of Suspension Stability on the Quality of the Spin Coated Zeolite Films

In order to demonstrate the effect of dispersion quality of suspensions on zeolite processing, PVP containing zeolite suspensions were spin-coated onto rectangle Si-wafer and glass substrates. For this application, the amount of solids loading is increased to 10 wt%.

The SEM micrographs of deposited zeolite suspensions on the Si-wafer were shown in Figure 4.14, in which top and side views of the coatings were compared for unstable and PEG-stabilized PVP containing LTA zeolites in ethanol:water (50:50 wt%) mixture. As shown in the Figure 4.14a and b the zeolite powders could not homogeneously cover the substrate surfaces, i.e., discontinuity was observed. Large empty areas on the substrate surface, as well as agglomerated areas were detected in the absence of PEG-400 molecules in suspensions. The empty regions were far higher than the average particle size of the treated zeolite powders.

On the other hand, denser films were observed using PEG-400 containing colloidal zeolite suspensions on the Si-wafer substrate. Only few small gaps were observed in Figure 4.14d and e, and the gaps were about in the range of particle size of the zeolite powders, which indicate the formation of close-packed zeolite films. Due to the small gaps, surface continuity was not excellent, but still, it was at a reasonable level and it could be further improved with optimization of the spin-coating and heating parameters.

As it can be observed in the Figure 4.14 c and f, the thicknesses of the films were more homogeneous when PEG-containing stabilized suspensions were used. Also, agglomerated zeolite powders were realized in the absence of the PEG molecules in Figure 4.14 c. As a result, spun coated zeolite films were indicator of the stability of the zeolite powders in the presence of PVP in ethanol:water (50:50 wt%) medium.

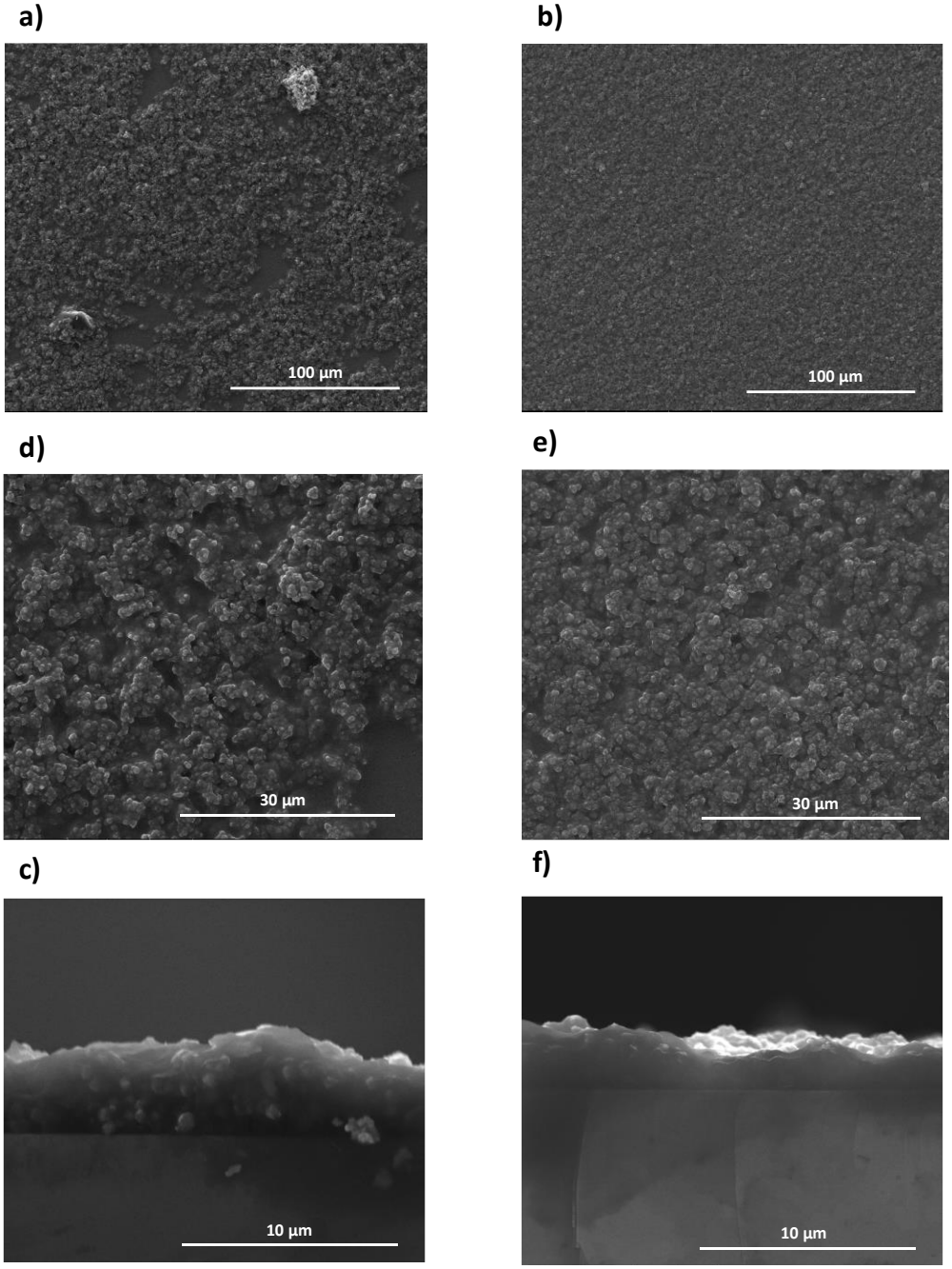

Figure 4.14. SEM micrographs of the LTA zeolite films by spin coating of the 10wt% zeolite powders in PVP added suspension in the absence (a,b, and c) and presence (d,e, and f) of PEG molecules in the ethanol-water (50:50 wt%) suspension on a Si wafer

CHAPTER 5

CONCLUSIONS AND RECOMMENDATIONS

5.1. Conclusions

The main aim of this study is to offer systematic investigation and improvement of the stability of LTA zeolites in ethanol-water mixed solvents in the absence and presence of carrier polymer of PVP.

For this reason, first as received powders were broken into smaller sizes via ball milling and ultrasonic treatments. As a result of the optimized process, all powders could be reduced into a colloidal size range (<1 μm).

Sedimentation measurements and zeta potential measurements of LTA zeolites in water surface charge of powder are high enough to ensure electrostatic stabilization. With the addition of ethanol in a solvent, the zeta potential values of LTA zeolites decreased and when 50 wt% ethanol was used, the surface charge was below the critical limit and powders sediment in a few hours.

In order to improve the stability of LTA zeolite powders in 50:50 wt% ethanol:water solutions, first, electrostatic stabilization mechanisms were studied. The chemical analysis and pH measurements showed that dissolution or ion exchange of zeolites, in suspensions with high ionic strength changes the chemical structure of the zeolites; therefore, electrostatic stabilization is not suggested for zeolite suspensions. Second, steric/electrosteric stabilization mechanisms were investigated for some LTA zeolite suspensions. Similarly, the use of polyelectrolytes did not improve the stability of suspensions. However, the use of nonionic additives, particularly PEG additions, leads to better stabilized suspensions. Zeta potential measurements and ATR-FTIR analysis showed that PEG molecules interact with LTA surfaces and increase the surface potential.

The stability of LTA zeolite powders in mixed solvents in the presence of carrier polymer was also investigated. ATR-FTIR analysis and zeta potential measurements showed that PVP molecules interact with LTA zeolite surface and decrease their zeta potential. This effect could be overcome with high initial zeta potential values in water rich solvents (ethanol:water ≤ 40 wt%); however, when ethanol ratio was increased to 50 wt%, the powders destabilized and sedimented. The addition of PEG molecules improved the stability in the presence of PVP as well. The ATR-FTIR analysis showed that both PEG and PVP interact the with LTA surface.

Lastly, the influence of suspension stability on the fabrication of the zeolite structures was demonstrated in the spin coated zeolite films. The PEG-stabilized PVP containing suspensions in ethanol-water mixed solvent lead to the formation of more uniform coatings with more homogeneously dispersed LTA zeolites with compared to the films produced form unstable suspensions.

5.2. Future Recommendations

The dispersion of LTA zeolites in the presence/absence of PVP in ethanol-water mixtures with PEG-400 molecules will be critical for colloidal processing of LTA zeolites in mixed solvents for production of high quality complex shaped zeolite structures. The formulations suggested in this study can be used for shape-forming via electrospinning, robocasting, or other novel zeolite processing techniques.

REFERENCES

[1] H. Van Bekkum, E.M. Flanigen, P.A. Jacobs, J.C. Jansen, Introduction to zeolite science and practice: Preface 1st edition, in: Stud. Surf. Sci. Catal., (2001). pp. 1-13.

[2] A.K. Cheetham, G. Férey, T. Loiseau, Open-Framework Inorganic Materials, Angew. Chemie Int. Ed. (1999).

[3] T. Montanari, E. Finocchio, E. Salvatore, G. Garuti, A. Giordano, C. Pistarino, G. Busca, CO_2 separation and landfill biogas upgrading: A comparison of 4A and 13X zeolite adsorbents, Energy. (2011).

[4] A.R. Loiola, J.C.R.A. Andrade, J.M. Sasaki, L.R.D. da Silva, Structural analysis of zeolite NaA synthesized by a cost-effective hydrothermal method using kaolin and its use as water softener, J. Colloid Interface Sci. (2012).

[5] A. Julbe, M. Drobek, Zeolite A Type, in: Encycl. Membr., 2016. pp. 1-2

[6] F. Collins, A. Rozhkovskaya, J.G. Outram, G.J. Millar, A critical review of waste resources, synthesis, and applications for Zeolite LTA, Microporous Mesoporous Mater. (2020).

[7] M. V. Opanasenko, W.J. Roth, J. Čejka, Two-dimensional zeolites in catalysis: Current status and perspectives, Catal. Sci. Technol. (2016).

[8] F. Rezaei, A. Mosca, J. Hedlund, P.A. Webley, M. Grahn, J. Mouzon, The effect of wall porosity and zeolite film thickness on the dynamic behavior of adsorbents in the form of coated monoliths, Sep. Purif. Technol. (2011).

[9] H. Thakkar, S. Eastman, A. Hajari, A.A. Rownaghi, J.C. Knox, F. Rezaei, 3D-Printed Zeolite Monoliths for CO_2 Removal from Enclosed Environments, ACS Appl. Mater. Interfaces. (2016).

[10] M.A. Snyder, M. Tsapatsis, Hierarchical nanomanufacturing: From shaped zeolite nanoparticles to high-performance separation membranes, Angew. Chemie - Int. Ed. (2007).

[11] J.C. Jansen, J.H. Koegler, H. Van Bekkum, H.P.A. Calis, C.M. Van Den Bleek, F. Kapteijn, J.A. Moulijn, E.R. Geus, N. Van Der Puil, Zeolitic coatings and their potential use in catalysis, Microporous Mesoporous Mater. (1998).

[12] N.L. Michels, S. Mitchell, M. Milina, K. Kunze, F. Krumeich, F. Marone, M. Erdmann, N. Marti, J. Pérez-Ramírez, Hierarchically structured zeolite bodies: Assembling micro-, meso-, and macroporosity levels in complex materials with enhanced properties, Adv. Funct. Mater. (2012).

[13] A. Zampieri, H. Sieber, T. Selvam, G.T.P. Mabande, W. Schwieger, F. Scheffler, M. Scheffler, P. Greil, Biomorphic cellular Si-SiC/zeolite ceramic composites: From rattan palm to bioinspired structured monoliths for catalysis and sorption, Adv. Mater. (2005).

[14] Saepurahman, G.P. Singaravel, R. Hashaikeh, Fabrication of electrospun LTL zeolite fibers and their application for dye removal, J. Mater. Sci. (2016).

[15] A. Ojuva, M. Järveläinen, M. Bauer, L. Keskinen, M. Valkonen, F. Akhtar, E. Levänen, L. Bergström, Mechanical performance and CO2 uptake of ion-exchanged zeolite A structured by freeze-casting, J. Eur. Ceram. Soc. (2015).

[16] S. Lawson, Q. Al-Naddaf, A. Krishnamurthy, M.S. Amour, C. Griffin, A.A. Rownaghi, J.C. Knox, F. Rezaei, UTSA-16 Growth within 3D-Printed Co-Kaolin Monoliths with High Selectivity for CO_2/CH_4, CO_2/N_2, and CO_2/H_2 Separation, ACS Appl. Mater. Interfaces. (2018).

[17] F. Akhtar, L. Bergström, Colloidal processing and thermal treatment of binderless hierarchically porous zeolite 13X monoliths for CO_2 capture, J. Am. Ceram. Soc. (2011).

[18] A. Ojuva, F. Akhtar, A.P. Tomsia, L. Bergström, Laminated adsorbents with very rapid CO_2 uptake by freeze-casting of zeolites, ACS Appl. Mater. Interfaces. (2013).

[19] W. Shan, Y. Zhang, W. Yang, C. Ke, Z. Gao, Y. Ye, Y. Tang, Electrophoretic deposition of nanosized zeolites in non-aqueous medium and its application in fabricating thin zeolite membranes, Microporous Mesoporous Mater. (2004).

[20] K. Namekawa, M. Tokoro Schreiber, T. Aoyagi, M. Ebara, Fabrication of zeolite-polymer composite nanofibers for removal of uremic toxins from kidney failure patients, Biomater. Sci. (2014).

[21] V. Pillay, C. Dott, Y.E. Choonara, C. Tyagi, L. Tomar, P. Kumar, L.C. Du Toit, V.M.K. Ndesendo, A review of the effect of processing variables on the fabrication of electrospun nanofibers for drug delivery applications, J. Nanomater. (2013).

[22] F.L. Toma, A. Potthoff, L.M. Berger, C. Leyens, Demands, Potentials, and Economic Aspects of Thermal Spraying with Suspensions: A Critical Review, J. Therm. Spray Technol. (2015).

[23] N.Z.A. Al-Hazeem, Nanofibers and Electrospinning Method, in: Nov. Nanomater. - Synth. Appl., (2018).

[24] C.J. Clarke, W.C. Tu, O. Levers, A. Bröhl, J.P. Hallett, Green and Sustainable Solvents in Chemical Processes, Chem. Rev. (2018).

[25] Y.C. Huang, W.J. Hsu, C.Y. Wang, H.K. Tsao, Y.H. Kang, J.J. Chen, D.Y. Kang, Wetting Properties and Thin-Film Quality in the Wet Deposition of Zeolites, ACS Omega. (2019).

[26] I.A. Aksay, Microstructure Control Through Colloidal Consolidation., in: Adv. Ceram., (1984), pp. 94-96.

[27] S. Chemistry, Coatings, Handbook of Applied Surface and Colloid Chemistry, Pigment Resin Technol. (2006).

[28] P.J. Lloyd, Particle Characterization., Chem. Eng. (New York). (1974).

[29] D. Walter, Primary Particles - Agglomerates - Aggregates, in: Nanomaterials, (2013).

[30] G. V. Franks, C. Tallon, A.R. Studart, M.L. Sesso, S. Leo, Colloidal processing: enabling complex shaped ceramics with unique multiscale structures, J. Am. Ceram. Soc. (2017).

[31] D. Bonn, W.K. Kegel, Stokes-Einstein relations and the fluctuation-dissipation theorem in a supercooled colloidal fluid, J. Chem. Phys. (2003).

[32] J.C. Chang, F.F. Lange, D.S. Pearson, J.P. Pollinger, Pressure Sensitivity for Particle Packing of Aqueous Al_2O_3 Slurries vs Interparticle Potential, J. Am. Ceram. Soc. (1994).

[33] J.A. Lewis, Colloidal Processing of Ceramics, J. Am. Ceram. Soc. (2004).

[34] J. Israelachvili, Intermolecular and Surface Forces, (2011), pp. 119.

[35] W.E. Lee, Ceramic processing and sintering, Int. Mater. Rev. (2012).

[36] Malvern Instruments, Zeta potential: An Introduction in 30 minutes, Zetasizer Nano Serles Tech. Note. MRK654-01. (2011).

[37] I.A. Larmour, K. Faulds, D. Graham, SERS activity and stability of the most frequently used silver colloids, J. Raman Spectrosc. (2012).

[38] D. Li, M.B. Müller, S. Gilje, R.B. Kaner, G.G. Wallace, Processable aqueous dispersions of graphene nanosheets, Nat. Nanotechnol. (2008).

[39] Y. Zhang, E. Yildirim, H.S. Antila, L.D. Valenzuela, M. Sammalkorpi, J.L. Lutkenhaus, The influence of ionic strength and mixing ratio on the colloidal stability of PDAC/PSS polyelectrolyte complexes, Soft Matter. (2015).

[40] D. Sun, S. Kang, C. Liu, Q. Lu, L. Cui, B. Hu, Effect of zeta potential and particle size on the stability of SiO_2 nanospheres as carrier for ultrasound imaging contrast agents, Int. J. Electrochem. Sci. (2016).

[41] T. Tadros, General Principles of Colloid Stability and the Role of Surface Forces, in: Colloids Interface Sci. Ser., (2010).

[42] D.H. Napper, A. Netschey, Studies of the steric stabilization of colloidal particles, J. Colloid Interface Sci. (1971).

[43] A. V. Kiselev, D.P. Poshkus, Advances In Colloid And Interface Science., Adv. Colloid Interface Sci. (1978).

[44] H.G. Pedersen, L. Bergström, Forces Measured between Zirconia Surfaces in Poly(acrylic acid) Solutions, J. Am. Ceram. Soc. (2004).

[45] N.S. Bell, T.C. Monson, C. Diantonio, Y. Wu, Practical colloidal processing of multication ceramics, J. Ceram. Sci. Technol. (2016).

[46] S.J. Park, M.K. Seo, Intermolecular Force, (2011). pp. 6-11.

[47] P. Somasundaran, S.C. Mehta, X. Yu, S. Krishnakumar, Colloid Systems and Interfaces Stability and Surfactant Adsorption, in: Handb. Surf. Colloid Chem., (2009).

[48] B. Faure, G. Salazar-Alvarez, L. Bergström, Hamaker constants of iron oxide nanoparticles, Langmuir. (2011).

[49] Basics of zeolites, in: Adv. Struct. Mater., (2016). pp. 13-17.

[50] J. Cejka, H. Van Bekkum, A. Corma, F. Schüth, Studies in Surface Science and Catalysis 168: Introduction to Zeolite science and practice, Stud. Surf. Sci. Catal. (2007).

[51] C. Baerlocher, L.B. McCusker, Database of Zeolite Structures, Available at: Http://Www.Iza-Structure.Org/Databases/. (2014).

[52] M. Nocita, A. Stevens, M. van Wesemael, B., Aitkenhead, M. Bachmann, B. Barthes, E.B. Dor, D.J. Brown, M. Clairotte, A. Csorba, P. Dardenne, J.A. DemattÃa, V. Genot, C. Guerrero, M. Knadel, L. Montanarella, C. Noon, L. Ramirez-Lopez, J. Wetterlind, Chapter Four - Soil Spectroscopy: An Alternative to Wet Chemistry for Soil Monitoring, Adv. Agron. (2015).

[53] Synthetic Zeolites Market by Type & Application - Global Forecast 2023 | MarketsandMarkets, (n.d.). https://www.marketsandmarkets.com/Market-Reports/synthetic-zeolite-market-74181103.html (accessed December 23, 2019).

[54] Reitmeier_Zeolites | Elite Netzwerk Bayern, (n.d.). https://www.elitenetzwerk.bayern.de/elitenetzwerk-home/forschungsarbeiten/naturwissenschaften/2009/reitmeier-zeolites/ (accessed December 23, 2019).

[55] L.V.C. Rees, Introduction to Zeolite Science and Practice, Zeolites. (1992), vol. 58.

[56] K. Ramesh, D.D. Reddy, A.K. Biswas, A.S. Rao, Zeolites and Their Potential Uses in Agriculture, Adv. Agron. (2011).

[57] A. Corma, H. Garcia, S. Iborra, J. Primo, ChemInform Abstract: Modified Faujasite Zeolites as Catalysts in Organic Reactions: Esterification of Carboxylic Acids in the Presence of HY Zeolites., ChemInform. (1990).

[58] S.R. Kirumakki, N. Nagaraju, S. Narayanan, A comparative esterification of benzyl alcohol with acetic acid over zeolites Hβ, HY and HZSM5, Appl. Catal. A Gen. (2004).

[59] P. Ferreira, I.M. Fonseca, A.M. Ramos, J. Vital, J.E. Castanheiro, Esterification of glycerol with acetic acid over dodecamolybdophosphoric acid encaged in USY zeolite, Catal. Commun. (2009).

[60] Y. Gao, B. Zheng, G. Wu, F. Ma, C. Liu, Effect of the Si/Al ratio on the performance of hierarchical ZSM-5 zeolites for methanol aromatization, RSC Adv. (2016).

[61] N. Kosinov, C. Auffret, G.J. Borghuis, V.G.P. Sripathi, E.J.M. Hensen, Influence of the Si/Al ratio on the separation properties of SSZ-13 zeolite membranes, J. Memb. Sci. (2015).

[62] J. Jiang, L. Peng, X. Wang, H. Qiu, M. Ji, X. Gu, Effect of Si/Al ratio in the framework on the pervaporation properties of hollow fiber CHA zeolite membranes, Microporous Mesoporous Mater. (2019).

[63] T. Kawai, K. Tsutsumi, Evaluation of hydrophilic-hydrophobic character of zeolites by measurements of their immersional heats in water, Colloid Polym. Sci. (1992).

[64] A. Bolshakov, D.E. Romero Hidalgo, A.J.F. van Hoof, N. Kosinov, E.J.M. Hensen, Mordenite Nanorods Prepared by an Inexpensive Pyrrolidine-based Mesoporogen for Alkane Hydroisomerization, ChemCatChem. (2019).

[65] LTA: Framework Type, (n.d.). https://asia.iza-structure.org/IZA-SC/framework.php?STC=LTA (accessed December 23, 2019).

[66] R.P. Townsend, E.N. Coker, Ion exchange in zeolites, in: Stud. Surf. Sci. Catal., (2001), pp. 480-482.

[67] B.W. Boal, J.E. Schmidt, M.A. Deimund, M.W. Deem, L.M. Henling, S.K. Brand, S.I. Zones, M.E. Davis, Facile Synthesis and Catalysis of Pure-Silica and Heteroatom LTA, Chem. Mater. (2015).

[68] A. Corma, F. Rey, J. Rius, M.J. Sabater, S. Valencia, Supramolecular self-assembled molecules as organic directing agent for synthesis of zeolites, Nature. (2004).

[69] T.H. Đặng, B.H. Chen, D.J. Lee, Optimization of biodiesel production from transesterification of triolein using zeolite LTA catalysts synthesized from kaolin clay, J. Taiwan Inst. Chem. Eng. (2017).

[70] C. Chen, W.S. Ahn, CO_2 adsorption on LTA zeolites: Effect of mesoporosity, Appl. Surf. Sci. (2014).

[71] F. Akhtar, L. Andersson, N. Keshavarzi, L. Bergström, Colloidal processing and CO_2 capture performance of sacrificially templated zeolite monoliths, Appl. Energy. (2012).

[72] S. Couck, J. Cousin-Saint-Remi, S. Van der Perre, G. V. Baron, C. Minas, P. Ruch, J.F.M. Denayer, 3D-printed SAPO-34 monoliths for gas separation, Microporous Mesoporous Mater. (2018).

[73] F.A. Hasan, P. Xiao, R.K. Singh, P.A. Webley, Zeolite monoliths with hierarchical designed pore network structure: Synthesis and performance, Chem. Eng. J. (2013).

[74] C. Matsunaga, T. Uchikoshi, T.S. Suzuki, Y. Sakka, M. Matsuda, Fabrication of the c-axis oriented zeolite L compacts using strong magnetic field, Mater. Lett. (2013).

[75] C. Matsunaga, T. Uchikoshi, T.S. Suzuki, Y. Sakka, M. Matsuda, Fabrication of c-axis-oriented zeolite L seed layer on porous zirconia substrate by electrophoretic deposition in strong magnetic field, in: Key Eng. Mater., 2015.

[76] J. Di, H. Chen, X. Wang, Y. Zhao, L. Jiang, J. Yu, R. Xu, Fabrication of zeolite hollow fibers by coaxial electrospinning, Chem. Mater. (2008).

[77] S.F. Anis, R. Hashaikeh, Electrospun zeolite-Y fibers: Fabrication and morphology analysis, Microporous Mesoporous Mater. (2016).

[78] US8216439B2 - Hybrid slip casting-electrophoretic deposition (EPD) process - Google Patents, (n.d.). https://patents.google.com/patent/US8216439B2/en (accessed December 23, 2019).

[79] J. Kobler, H. Abrevaya, S. Mintova, T. Bein, High-silica zeolite-β: From stable colloidal suspensions to thin films, J. Phys. Chem. C. (2008).

[80] L.H. Wee, L. Tosheva, C. Vasilev, A.M. Doyle, Influence of the dispersion medium on the properties of spin-coated Silicalite-1 films, Microporous Mesoporous Mater. (2007).

[81] Z.V. Feng, W.S. Chen, K. Keratithamkul, M. Stoick, B. Kapala, E. Johnson, A.C. Huang, T.Y. Chin, Y.W. Chen-Yang, M.L. Yang, Degradation of the electrospun silica nanofiber in a biological medium for primary hippocampal neuron – effect of surface modification, Int. J. Nanomedicine. (2016).

[82] K.F.L. Hagesteijn, S. Jiang, B.P. Ladewig, A review of the synthesis and characterization of anion exchange membranes, J. Mater. Sci. (2018).

[83] D.T.W. Toolan, S. Fujii, S.J. Ebbens, Y. Nakamura, J.R. Howse, On the mechanisms of colloidal self-assembly during spin-coating, Soft Matter. (2014).

[84] Q. Chen, L. Cordero-Arias, J.A. Roether, S. Cabanas-Polo, S. Virtanen, A.R. Boccaccini, Alginate/Bioglass® composite coatings on stainless steel deposited by direct current and alternating current electrophoretic deposition, Surf. Coatings Technol. (2013).

[85] B. Ouedraogo, Electrophoretic Deposition of Alumina and Nickel Oxide Particles, J. Sci. Res. Reports. (2013).

[86] S. Ling, R. Yuan, Y. Chai, T. Zhang, Study on immunosensor based on gold nanoparticles/chitosan and MnO_2 nanoparticles composite membrane/Prussian blue modified gold electrode, Bioprocess Biosyst. Eng. (2009).

[87] D. Schiemann, P. Alphonse, P.L. Taberna, Synthesis of high surface area TiO_2 coatings on stainless steel by electrophoretic deposition, J. Mater. Res. (2013).

[88] A.E.W. Beers, T.A. Nijhuis, N. Aalders, F. Kapteijn, J.A. Moulijn, BEA coating of structured supports - Performance in acylation, Appl. Catal. A Gen. (2003).

[89] W. Zhang, K. Narang, S.B. Simonsen, N.M. Vinkel, M. Gudik-Sørensen, L. Han, F. Akhtar, A. Kaiser, Highly Structured Nanofiber Zeolite Materials for Biogas Upgrading, Energy Technol. (2019).

[90] J. Seo, U. Paik, Preparation and characterization of slurry for chemical mechanical planarization (CMP), in: Adv. Chem. Mech. Planarization, (2016).

[91] H. Ohtsuka, H. Mizutani, S. Iio, K. Asai, T. Kiguchi, H. Satone, T. Mori, J. Tsubaki, Effects of sintering additives on dispersion properties of Al_2O_3 slurry containing polyacrylic acid dispersant, J. Eur. Ceram. Soc. (2011).

[92] D. Santhiya, S. Subramanian, K.A. Natarajan, S.G. Malghan, Surface chemical studies on the competitive adsorption of poly(acrylic acid) and poly(vinyl alcohol) onto alumina, J. Colloid Interface Sci. (1999).

[93] S. Liufu, H. Xiao, Y. Li, Adsorption of poly(acrylic acid) onto the surface of titanium dioxide and the colloidal stability of aqueous suspension, J. Colloid Interface Sci. (2005).

[94] K.H. Bu, B.M. Moudgil, Selective chemical mechanical polishing using surfactants, J. Electrochem. Soc. (2007).

[95] J.E. Hampsey, C.L. De Castro, B. McCaughey, D. Wang, B.S. Mitchell, Y. Lu, Preparation of micrometer- to sub-micrometer-sized nanostructured silica particles using high-energy ball milling, J. Am. Ceram. Soc. (2004).

[96] L. Song, R. Zhang, L. Mao, W. Zhu, M. Zheng, Influence of different dispersants on the dispersion property of nano-aluminium powders, in: Appl. Mech. Mater., (2011).

[97] Z. Liu, J. Zhu, T. Wakihara, T. Okubo, Ultrafast synthesis of zeolites: Breakthrough, progress and perspective, Inorg. Chem. Front. (2019).

[98] L. Gabrielson, M.J. Edirisinghe, On the dispersion of fine ceramic powders in polymers, J. Mater. Sci. Lett. (1996).

[99] B. Peng, Y. Huang, L.Y. Chai, G.L. Li, M.M. Cheng, X.F. Zhang, Influence of polymer dispersants on dispersion stability of nano-TiO 2 aqueous suspension and its application in inner wall latex paint, J. Cent. South Univ. Technol. (English Ed. (2007).

[100] W. Zhao, D.A. Yang, X.X. Yin, T.X. Xu, Study on Stability of Nano-Al_2O_3 Aqueous Suspension, Key Eng. Mater. (2007).

[101] X. Teng, H. Liu, C. Huang, Effect of Al_2O_3 particle size on the mechanical properties of alumina-based ceramics, Mater. Sci. Eng. A. (2007).

[102] H. Shin, S. Lee, H. Suk Jung, J.B. Kim, Effect of ball size and powder loading on the milling efficiency of a laboratory-scale wet ball mill, Ceram. Int. (2013).

[103] J. Li, A. Corma, J. Yu, Synthesis of new zeolite structures, Chem. Soc. Rev. (2015).

[104] J.H. Adair, E. Suvaci, Submicron Electroceramic Powders by Hydrothermal Synthesis, in: Encycl. Mater. Sci. Technol., (2001).

[105] T.W. Kirk, S.G. Caldwell, J.J. Oakes, Mo-Cu composites for electronic packaging applications, in: Adv. Powder Metall., (1992).

[106] R.L. Hartman, H.S. Fogler, Understanding the dissolution of zeolites, Langmuir. (2007).

[107] S. Yamamoto, S. Sugiyama, O. Matsuoka, K. Kohmura, T. Honda, Y. Banno, H. Nozoye, Dissolution of zeolite in acidic and alkaline aqueous solutions as revealed by AFM imaging, J. Phys. Chem. (1996).

[108] M. Król, W. Mozgawa, W. Jastrzbski, K. Barczyk, Application of IR spectra in the studies of zeolites from D4R and D6R structural groups, Microporous Mesoporous Mater. (2012).

[109] C. Feng, K.C. Khulbe, T. Matsuura, R. Farnood, A.F. Ismail, Recent progress in zeolite/zeotype membranes, J. Membr. Sci. Res. (2015).

[110] H. Thakkar, S. Lawson, A.A. Rownaghi, F. Rezaei, Development of 3D-printed polymer-zeolite composite monoliths for gas separation, Chem. Eng. J. (2018).

[111] X. Wu, X. Yang, H. Yang, Z. Guo, J. Lin, W. Wu, X. Liang, Y. He, Hierarchically structured PVP porous fibers derived from the embedding of NaY zeolite synergize the adsorption of benzene, Compos. Part B Eng. (2019).

[112] C.S. Ramya, S. Selvasekarapandian, G. Hirankumar, T. Savitha, P.C. Angelo, Investigation on dielectric relaxations of PVP-NH4SCN polymer electrolyte, J. Non. Cryst. Solids. (2008).

[113] N. Soltani, E. Saion, M. Erfani, K. Rezaee, G. Bahmanrokh, G.P.C. Drummen, A. Bahrami, M.Z. Hussein, Influence of the polyvinyl pyrrolidone concentration on particle size and dispersion of ZnS nanoparticles synthesized by microwave irradiation, Int. J. Mol. Sci. (2012).

APPENDIX A: Settling Behavior of LTA Zeolite Powder

Table A.1 Settling velocity of the zeolite with respect to particle diameter in Ethanol:Water (50:50 wt%) by Stoke's law refinement

d (μm)	hour	distance x(mm)	V (mm/h)
1.98	*0.50*	*5*	*10.0*
0.99	*2.00*	*5*	*1.67*
0.05	*6.00*	*5*	*0.83*
0.04	*11.00*	*5*	*0.45*
0.03	*18.00*	*5*	*0.28*

APPENDIX B: FTIR Analysis of PVP molecules in Ethanol:Water solution

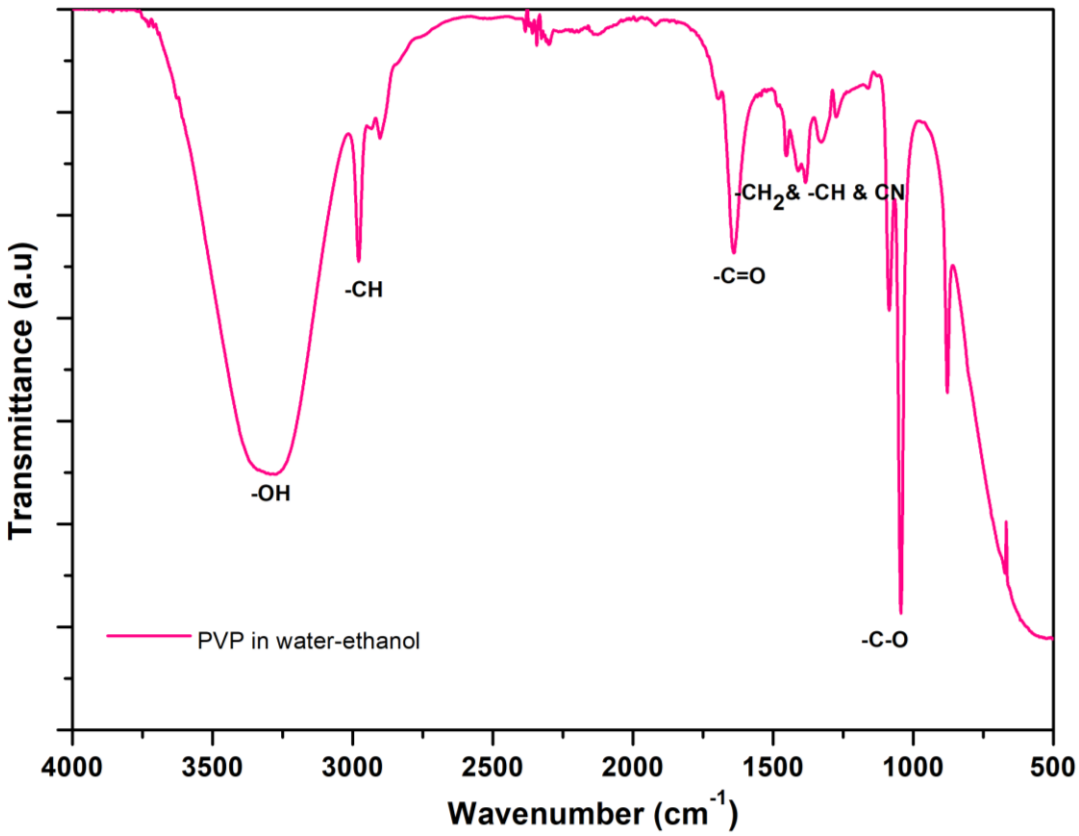

Figure B.1. ATR-FTIR spectrum of PVP molecules in Ethanol:Water (50:50 wt%) media